23 QUANTUM THEORY OF THE LASER

János A. Bergou[a,b]
Berthold-Georg Englert[a,c,d]
Melvin Lax[e,*]
Marian O. Scully[a,c]
Herbert Walther[c,f,*]
M. Suhail Zubairy[a,g]

[a]*Institute for Quantum Studies and Department of Physics*
Texas A&M University
College Station, Texas

[b]*Department of Physics and Astronomy*
Hunter College of the City University of New York
New York, New York

[c]*Max-Planck-Institut für Quantenoptik*
Garching bei München, Germany

[d]*Abteilung Quantenphysik der Universität Ulm*
Ulm, Germany

[e]*Department of Physics*
City College of the City University of New York
New York, New York

[f]*Sektion Physik der Universität München*
Garching bei München, Germany

[g]*Department of Electronics*
Quaid-i-Azam University
Islamabad, Pakistan

23.1 GLOSSARY

Section 23.3

$a_k, a_k^\dagger$	annihilation, creation operator for photons in the kth mode
A	Einstein coefficient for spontaneous emission
$\mathbf{A}_k(\mathbf{r})$	kth electric mode function at position $\mathbf{r}$

*Deceased.

B	Einstein coefficient for absorption and stimulated emission
$\mathbf{B}(\mathbf{r}, t)$	magnetic field at position $\mathbf{r}$ and time t
$\mathbf{B}_k(\mathbf{r})$	kth magnetic mode function at position $\mathbf{r}$
c	speed of light
$\mathbf{e}_k$	polarization unit vector of the kth mode
$\mathbf{E}_\perp(\mathbf{r}, t)$	transverse electric field at position $\mathbf{r}$ and time t
$h, \hbar$	*Planck's constant* $[\hbar = h/(2\pi)]$
$\mathbf{k}, k$	wave vector, its length
$(d\mathbf{k})$	three-dimensional volume element in $\mathbf{k}$ space
k_B	Boltzmann's constant
$\mathbf{n}_k$	propagation unit vector of the kth mode
N	photon number operator
N_e	number of excited-state atoms
N_g	number of ground-state atoms
$\mathbf{r}$	position vector
$(d\mathbf{r})$	three-dimensional volume element in $\mathbf{r}$ space
t, dt	time, time interval
T	temperature
U_{1ph}	energy density for a one-photon state
dV	volume element
$\lvert\mathbf{vac}\rangle, \langle\mathbf{vac}\rvert$	ket and bra of the photon vacuum
$\overline{w^2}$	mean square energy fluctuations
W	spectral-spatial energy density of blackbody radiation
α_k	coherent state amplitudes
$\lvert\{\alpha\}_c\rangle$	ket of a coherent state
δ_{jk}	Kronecker's delta symbol
$\delta_\perp(\mathbf{r})$	transverse delta function at $\mathbf{r}$ (a dyadic)
ε_0	dielectric constant $[\varepsilon_0 = 1/(\mu_0 c^2) \simeq 8.854 \times 10^{-2}\ \mathrm{F/m}]$
μ_0	permeability constant $(4\pi \times 10^{-7}\ \mathrm{H/m})$
$\nu, d\nu$	light frequency, frequency interval
ν_k	frequency of the kth mode
ϱ_{ph}	statistical operator of the photon field
ρ	probability amplitude for reflection
τ	probability amplitude for transmission
ψ_k, ψ_{jk}	probability amplitudes of the one-photon, two-photon states
$\lvert\{\psi\}_1\rangle, \lvert\{\psi\}_2\rangle$	kets for one-photon, two-photon states
∇	gradient vector differential operator

Section 23.4

A	destruction operator for the field
$\mathscr{A}$	laser gain coefficient
$a, a^\dagger$	photon ladder operators
$\mathscr{B}$	laser saturation parameter
$b_k, b_k^\dagger$	destruction and creation operators for the reservoir modes
$\mathscr{D}$	largest eigenvalue of the laser equation

QUANTUM THEORY OF THE LASER 23.3

$F(t)$	field noise operator
$F_\alpha(t), F_\gamma$	noise operators associated with gain and loss, respectively
$F(1, x, y)$	hypergeometric function
g	radiant frequency stating the strength of atom-photon coupling
g_k	couping coefficient between reservoir and field
$G^{(1)}(t_0 + t, t_0)$	field correlation function
$\mathcal{H}, \mathcal{H}_0, \mathcal{H}_1$	total, free, and interaction hamiltonians for atom-field interaction
k	wave vector for the field
K	kick operator
$\mathcal{L}$	superoperator for cavity damping
$M(\tau)$	superoperator describing the effect of a single inverted atom on the field
$\overline{n}, \overline{n^2}$	mean and mean squared number of photons in a laser
n_m	maximum of the photon distribution of a laser
n_{th}	mean number of photons in a thermal reservoir
N_{ex}	number of atoms traversing the cavity during the lifetime of the cavity field
$N(t_i, t, \tau)$	notch function
p	transition dipole moment
$p(n)$	photon distribution function
$P(\tau)$	distribution function for the interaction times
q	a nonnegative integer
Q	Mandel Q function
r	atom injection rate inside a laser and micromaser
$S(\omega)$	spectrum of the laser field
T	temperature
t_m	measurement time
U	time evolution operator
$U_{\text{af}}(\tau)$	atom-field time evolution operator
$\mathcal{V}$	interaction picture Hamiltonian
$\alpha(t, t')$	gain function of a laser
Γ	atomic decay rate via spontaneous emission
$\gamma, \gamma_a, \gamma_b$	atomic decay rates
$\delta_{nn'}$	Kronecker delta function
ν_k	frequency of the reservoir mode
σ_+, σ_-	ladder operators for a two-level atom
σ_z	atomic inversion operator
ω_0	radiant frequency of an atomic transition
λ	eigenvalue
λ_j	eigenvalues of the laser equation
$\rho(t)$	reduced density operator for the field
ρ_{at}	total density operator for the atom-field system
$\rho_{nn'}$	matrix elements of the field density operator
$\rho_n^{(k)}$	off-diagonal density matrix element
κ	cavity loss rate
χ	square of the ratio of vacuum Rabi frequency and the atomic decay rate
$\theta(t)$	step function
$\phi(t)$	phase of the field

Section 23.5

a, b, c, d	parameters appearing in Table 1
E	electric field strength
$\overline{E}$	mean field
$F(M), F_0$	free energy of a ferromagnet, its value for $M = 0$
g_k	undefined in Eqs. (126) and (127)
$G(E), G_0$	free energy of a laser, its value for $E = 0$
H	external magnetic field
H_{n0}	heating rate
K	one-fourth the spontaneous emission rate
K_{n0}	cooling rate
n_0	number of atoms in the Bose-Einstein condensate
$\langle n_0 \rangle$	mean number of atoms in the condensate
$\langle \dot{n}_0 \rangle$	time derivative of $\langle n_0 \rangle$
$\langle n_k \rangle_{n_0}$	average number of atoms in the kth excited state, given n_0 atoms in the condensate
N	total number of Bose atoms
N', N''	normalization constants in Table 1
M	magnetization of a ferromagnet
$P(M)$	probability density for a ferromagnet
$P(E)$	probability density for a laser
$P(\alpha, \alpha^*)$	P representation for the field
S	injected signal
T_c	critical temperature
W_k	heat bath density of states
x, y	$x = \text{Re } \alpha, y = \text{Im } \alpha$
X	zero-field susceptibility of a ferromagnet
$Z(T, N)$	canonical partition function
α	eigenvalue of the coherent state $\lvert\alpha\rangle$
ε	scaled temperature (inversion) of a ferromagnet (laser) in Fig. 9
$\zeta(3)$	Riemann's zeta function $\zeta(3) = 1.2020569 \ldots$
η	scaled thermodynamical variable (in Fig. 9)
$\langle \eta_k \rangle$	average occupation number of the kth heat bath oscillator
$\Theta(\ )$	Heaviside's unit step function
$\mathbf{k}$	undefined in Eq. (15)
ξ	laser analog of X
$\rho_{n0,\,n0}$	probability for having n_0 atoms in the condensate
$\dot{\rho}_{n0,\,n0}$	time derivative of $\rho_{n0,\,n0}$
σ	population inversion
σ_t	threshold inversion
$\Phi_e(\eta)$	scaled thermodynamical potential (in Fig. 9)
Ω	trap frequency

Section 23.6

A	phase-shifted destruction operator for a free-electron laser (FEL)
c_b, c_c	probability amplitudes for atom to be in levels $\lvert b\rangle$ and $\lvert c\rangle$, respectively

QUANTUM THEORY OF THE LASER 23.5

$\mathcal{D}(\theta)$	phase diffusion function
$\mathcal{E}$	slowly varying field amplitude
g	coupling constant for the electron-field interaction in an FEL
j	parameter for the gain in an FEL
k	wavevector for the laser field in an FEL
$\mathcal{L}$	linear gain $(i = j)$ and cross-coupling $(i \neq j)$ Liouville operators
m	mass of electron
$O(A, A^\dagger)$	arbitrary operator containing A, $A^\dagger$
p	electron momentum
$\overline{p}$	eigenvalue of electron momentum operator
P_b, P_c	probability of atom being in states $\lvert b\rangle$ and $\lvert c\rangle$, respectively
P_{emission}	probability of emission of radiation
$S(T)$	time-evolution operator for the electron-photon state
T	electron-photon interaction time
$\mathcal{T}$	time-ordering operator
z	electron coordinate
α_i	eigenvalue of the coherent state $\lvert\alpha_i\rangle$
α_{ij}	constants depending upon parameters of gain medium in a correlated emission laser (CEL)
β	normalized electron momentum
γ	relativistic factor for an electron
Δ	atom-field detuning in lasing without inversion (LWI)
ν_1, ν_2	frequencies of the two modes in a CEL
$\rho(t_i)$	atomic density operator at initial time t_i
$\rho_{ij}^{(0)}$	initial values of the ijth atomic matrix elements
ρ_i	classical amplitude of the ith mode
$\rho(a_1, a_1^\dagger; a_2, a_2^\dagger)$	reduced density operator for the two-mode field in a CEL
θ_i	phase of the ith field
ω_0	microwave frequency
ω_a, ω_b, ω_c	frequencies associated with atomic levels
λ_s	wavelength of the field emitted in an FEL
λ_w	the period of the magnetic wiggler
κ	gain coefficient
$\kappa_{a\to b}$, $\kappa_{a\to c}$	constants depending upon the matrix elements between the relevant levels
ϕ	relative phase between atomic levels
Φ	total phase angle in two-mode CEL schemes
ψ	relative phase $\Phi + \theta_1 - \theta_2$

23.2 INTRODUCTION

Most lasers, and in particular all commercially sold ones, emit electromagnetic radiation whose properties can be accounted for quite well by a *semiclassical* description. In such a treatment, quantum aspects (level spacings, oscillator strengths, etc.) of the matter (atoms, molecules, electron-hole pairs, etc.) that constitute the gain medium are essential, but those of the electromagnetic field are disregarded. Quantum properties of the radiation are, however, of decisive importance for laser systems "at the limit" which reach fundamental bounds for the linewidth, for the regularity of photon statistics, or for other quantities of interest.

Recognition and understanding of these fundamental limitations are furnished by the quantum theory of the laser, whose foundations were laid in the 1960s. The two main approaches, the master-equation formalism and the Langevin method—equivalent in the physical contents and supplementing each other like spouses—can be roughly, and somewhat superficially, associated with the Schrödinger and the Heisenberg pictures of quantum mechanics. The master-equation method corresponds to the former, the Langevin approach to the latter. Both are reviewed in Sec. 23.4, but more room is given to the master-equation treatment. This bias originates in our intention to present a parallel exposition for both the standard laser theory and the theory of the micromaser, which in turn is traditionally and most conveniently treated by master equations.

The micromaser, in which the dynamic is dominated by the strong coupling of a single mode of the radiation field to a single atomic dipole transition, is the prototype of an open, driven quantum system. Accordingly, micromaser experiments are *the* test ground for the quantum theory of the laser; therefore, micromaser theory deserves the special attention that it receives in Sec. 23.4.

As a logical and historical preparation, we recall in Sec. 23.3, the theoretical and experimental facts that are evidence for quantum properties of electromagnetic radiation in general, and the reality of photons in particular. Some special issues are discussed in Sees. 23.5 and 23.6. In Sec. 23.5, we stress the analogy between the threshold behavior of a laser and the phase transition of a ferromagnet, and note the recent lessons about Bose-Einstein condensates taught by this analogy. Section 23.6 summarizes the most important features of some exotic lasers and masers, which exploit atomic coherences or the quantum properties of the atomic center-of-mass motion. Basics of the so-called free-electron laser are reported as well.

The quantum theory of the laser is a central topic in the field of quantum optics. An in-depth understanding of the various facets of quantum optics can be gained by studying the pertinent textbooks.[1–18]

23.3 SOME HISTORY OF THE PHOTON CONCEPT

Early History: Einstein's Light Quanta

Planck's formula of 1900[19] marks the beginning of quantum mechanics, and in particular of the quantum theory of light. It reads

$$W = \frac{8\pi\nu^2}{c^3}\frac{h\nu}{\exp(h\nu/k_B T)-1} \tag{1}$$

and relates the spectral-spatial energy density W of blackbody radiation to the frequency ν of the radiation and the temperature T of the blackbody. Boltzmann's constant k_B and Planck's constant h are conversion factors that turn temperature and frequency into energy, and c is the speed of light. A volume dV contains electromagnetic energy of the amount $W\,d\nu\,dV$ in the frequency range $\nu \cdots \nu + d\nu$.

The first factor in Eq. (1) is the density of electromagnetic modes. It obtains as a consequence of the classical wave theory of light and owes its simplicity to an implicit short-wavelength approximation. For wavelengths of the order of magnitude set by the size of the cavity that contains the radiation, appropriate corrections have to be made that reflect the shape and size of the cavity. This is of great importance in the context of micromasers, but need not concern us presently.

The second factor in Eq. (1) is the mean energy associated with radiation of frequency ν. It is a consequence of the quantum nature of light. In the limits of very high frequencies or very low ones, it turns into the respective factors of Wien[20] and Rayleigh-Jeans:[21,22]

$$\begin{aligned} &\frac{h\nu}{\exp(h\nu/k_B T)-1} && \text{(Planck)} \\ \to &\begin{cases} h\nu\exp-\dfrac{h\nu}{k_B T} & \text{for } \nu \gg \dfrac{k_B T}{h} \quad \text{(Wien)} \\ k_B T & \text{for } \nu \ll \dfrac{k_B T}{h} \quad \text{(Rayleigh-Jeans)} \end{cases} \end{aligned} \tag{2}$$

The relevant frequency scale is set by $k_B T/h$; at a temperature of $T = 288$ K it is about 6×10^{12} Hz, corresponding to a wavelength of 50 μm.

Ironically, Planck—whose stroke of genius was to interpolate between the two limiting forms of Eq. (2)—was not convinced of the quantum nature of electromagnetic radiation until much later. Legend has it that it was the discovery of Compton scattering in 1923 that did it.[23] We are, however, getting ahead of the story.

The true significance of Planck's formula, Eq. (1), started to emerge only after Einstein[24] had drawn the conclusions that led him to his famous *light-quantum hypothesis* of 1905, the *annus mirabilis*. In Pauli's words,

> He immediately applied [it] to the photoelectric effect and to Stokes' law for fluorescence, later also to the generation of secondary cathode rays by X-rays and to the prediction of the high frequency limit in the *Bremsstrahlung*.[25]

Quite a truckload, indeed.

The conflict with the well-established wave theory of light was, of course, recognized immediately, and so the introduction of light quanta also gave birth to the wave-particle duality. Upon its extension to massive objects by de Broglie in 1923 to 1924,[26–27] it was instrumental in Schrödinger's wave mechanics.[28]

Taylor's 1909 experiment,[29] in which feeble light produced interference fringes, although at most one light quantum was present in the interferometer at any time, addressed the issue of wave-particle duality from a different angle. Its findings are succinctly summarized in Dirac's dictum that "a photon interferes only with itself"[30]—a statement that became the innocent victim of misunderstanding and misquotation in the course of time.[31]

Another important step was taken the same year by Einstein.[32] By an ingenious application of thermodynamic ideas to Planck's formula, in particular consequences of Boltzmann's relation between entropy and statistics, he derived an expression for the mean-square energy fluctuations $\overline{w^2}$ of the radiation in a frequency interval $\nu \cdots \nu + d\nu$ and a volume dV:

$$\overline{w^2} = \left(\frac{c^3}{8\pi\nu^2} W + h\nu \right) W \, d\nu \, dV \tag{3}$$

where W is the spectral-spatial density of Eq. (1), so that $W \, d\nu \, dV$ is the mean energy in the frequency interval and volume under consideration. The first term is what one would get if classical electrodynamics accounted for all properties of radiation. There is no room for the second term in a wave theory of light; it is analogous to the fluctuations in the number of gas molecules occupying a given volume. This second term therefore supports Einstein's particle hypothesis of 1905,[24] in which electromagnetic energy is envisioned as being concentrated in localized lumps that are somehow distributed over the volume occupied by the electromagnetic wave.

Wave aspects (first term) and particle aspects (second term) enter Eq. (3) on equal footing. Since the thermodynamic considerations have no bias toward either one, one must conclude that Planck's formula, Eq. (1), is unbiased as well. Electromagnetic radiation is as much a particle phenomenon as it is a wave phenomenon.

Einstein left the center stage of quantum theory for some years, returning to it after completing his monumental work on general relativity. In 1913, Bohr's highly speculative postulates[33] had suddenly led to a preliminary understanding of many features of atomic spectra (the anomalous Zeeman effect was one big exception; it remained a bewildering puzzle for another decade). In the course, "quantum theory was liberated from the restriction to such particular systems as Planck's oscillators" (Pauli[25]).

Here was the challenge to rederive Planck's formula from Bohr's postulates, assuming that they hold for arbitrary atomic systems. Einstein's famous paper of 1917[34] accomplished just that, and more.

He considered radiation in thermal equilibrium with a dilute gas of atoms at temperature T. We shall here give a simplified treatment that contains the essential features without accounting for all

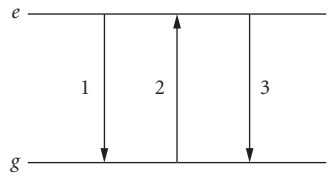

FIGURE 1 Transitions of three kinds happen between the excited level *e* and the ground level *g*: (1) spontaneous emission [see Eq. (4)], (2) absorption [see Eq. (5)], and (3) stimulated emission [see Eq. (6)].

details of lesser significance. Suppose that the energy spacing between two atomic levels *e* and *g* equals $h\nu$, so that the transition from the more energetic level *e* to the energetically lower level *g* (excited to ground state) is accompanied by the emission of a light quantum of frequency ν. According to Einstein, three processes are to be taken into account (see Fig. 1): spontaneous emission, absorption, and stimulated emission. The latter has no analog in Maxwell's electrodynamics.

Each of the three processes leads to a rate of change of the number of gas atoms in states *e* and *g*. Denoting these numbers by N_e and N_g we have the following contributions to their time derivatives. The *spontaneous emission* rate is proportional to the number of excited-state atoms:

Spontaneous emission
$$\frac{d}{dt}Ne = -\frac{d}{dt}N_g = -AN_e \tag{4}$$

where *A* is the first Einstein coefficient of the transition in question. The *absorption* rate is proportional to the number of ground-state atoms and to the energy density *W* of the radiation:

Absorption
$$\frac{d}{dt}N_e = -\frac{d}{dt}N_g = BWN_g \tag{5}$$

where *B* is the second Einstein coefficient. The *stimulated emission* rate is proportional to the number of excited state atoms and to the radiation energy density:

Stimulated emission
$$\frac{d}{dt}N_e = -\frac{d}{dt}N_g = BWN_e \tag{6}$$

where the same *B* coefficient appears as in the absorption rate.

The *detailed balance* between states *e* and *g* therefore requires

Total
$$\frac{d}{dt}Ne = -\frac{d}{dt}N_g = -AN_e + BWN_g - BWN_e = 0 \tag{7}$$

under the circumstances of thermal equilibrium. Therefore, *W* can be expressed in terms of the ratios A/B and N_g/N_e:

$$W = \frac{A/B}{N_g/N_e - 1} = \frac{A/B}{\exp(h\nu/k_B T) - 1} \tag{8}$$

where the second equality recognizes that Boltzmann's factor relates N_e to N_g. [The absence of additional weights here is the main simplification alluded to before; if taken into account, these weights would also require two closely related *B* coefficients in Eqs. (5) and (6).] In Eq. (8) we encounter the

denominator of Planck's factor from Eq. (2), and Planck's formula, Eq. (1), is recovered in full if the relation

$$A = \frac{8\pi h\nu^3}{c^3} B \tag{9}$$

is imposed on Einstein's coefficients.

The main ingredients in this derivation of Eq. (1) are the postulate of the process of stimulated emission, with a strength proportional to the density of radiation energy, and the relation between the coefficients for spontaneous emission and stimulated emission, Eq. (9).

All of this is well remembered, but there was in fact more to the 1917 paper.[34] It also contains a treatment of the momentum exchange between atoms and light quanta, and Einstein succeeded in demonstrating that the Maxwell velocity distribution of the atoms is consistent with the recoil they suffer when absorbing and emitting quanta. Insights gained in his study of Brownian motion (another seminal paper of 1905[35]) were crucial for this success. When taken together, the considerations about energy balance and those concerning momentum balance are much more convincing than either one could have been alone.

The discovery of the Compton effect in 1923[23] finally convinced Bohr and other skeptics of the reality of the particlelike aspects possessed by light. But Bohr, who until then was decidedly opposed to Einstein's light-quantum hypothesis and the consequent wave-particle duality, did not give in without a last try. Together with Kramers and Slater,[36] he hypothesized that perhaps energy-momentum conservation does not hold for each individual scattering event, but only in a statistical sense for a large ensemble. Then one could account for Compton's data without conceding a particle nature to light in general, and X rays in particular. The refined measurements that were immediately carried out by Bothe and Geiger[37] showed, however, that this hypothesis is wrong: energy and momentum are conserved in each scattering event, not just statistically.

And then there was, also in 1924, Bose's seminal observation that it is possible to derive Planck's radiation law [Eq. (1)] from purely corpuscular arguments without invoking at all the wave properties of light resulting from Maxwell's field equations.[38,39] The main ingredient in Bose's argument was the indistinguishability of the particles in question and a new way of counting them—now universally known as *Bose-Einstein statistics*—which pays careful attention to what is implied by their being indistinguishable. In the case of light quanta, an additional feature is that their number is not conserved, because light is easily emitted and absorbed. Massive particles (atoms, molecules, etc.), by contrast, are conserved; therefore, as Einstein emphasized,[40–42] their indistinguishability has further consequences, of which the phenomenon of Bose-Einstein condensation (or should one rather say "Einstein condensation of a Bose gas"?) is the most striking one.

Quantum Electrodynamics

Theoretical studies of the quantum nature of light had a much more solid basis after Dirac's introduction of quantum electrodynamics (QED) in his seminal paper of 1927.[43] The basic ingredients of QED were all present in Dirac's formulation, although it is true that a consistent understanding of QED was not available until renormalized QED was developed 20 years later (see the papers reprinted in Ref. 44). In particular, the photon concept was clarified in the sense described in the following paragraphs.

The infinite number of degrees of freedom of the electromagnetic field—an operator field in QED—become manageable with the aid of a mode expansion. For the transverse part $\mathbf{E}_\perp(\mathbf{r}, t)$ of the electric field, for example, it reads

$$\mathbf{E}_\perp(\mathbf{r}, t) = \sum_k \sqrt{\frac{h\nu_k}{2\varepsilon_0}} [a_k(t)\mathbf{A}_k(\mathbf{r}) + a_k^\dagger(t)\mathbf{A}_k^*(\mathbf{r})] \tag{10}$$

The mode functions $\mathbf{A}_k(\mathbf{r})$ are complex vector functions of the position vector $\mathbf{r}$ that are eigenfunctions of the Laplace differential operator,

$$-\nabla^2\mathbf{A}_k(\mathbf{r})=\left(\frac{2\pi\nu_k}{c}\right)^2\mathbf{A}_k(\mathbf{r}) \tag{11}$$

where the eigenvalue is determined by the frequency ν_k (>0) of the mode in question. The boundary conditions that the electric and magnetic field must obey at conducting surfaces imply respective boundary conditions on the $\mathbf{A}_k(\mathbf{r})$s.

The corresponding mode expansion for the magnetic field is given by

$$\mathbf{B}(\mathbf{r},t)=\sum_k\sqrt{\frac{\mu_0 h\nu_k}{2}}[-ia_k(t)\mathbf{B}_k(\mathbf{r})+ia_k^\dagger(t)\mathbf{B}_k^*(\mathbf{r})] \tag{12}$$

where

$$\mathbf{B}_k(\mathbf{r})=\frac{c}{2\pi\nu_k}\nabla\times\mathbf{A}_k(\mathbf{r});\qquad \mathbf{A}_k(\mathbf{r})=\frac{c}{2\pi\nu_k}\nabla\times\mathbf{B}_k(\mathbf{r}) \tag{13}$$

relates the two kinds of mode functions to each other.

Among others, the mode functions $\mathbf{A}_k(\mathbf{r})$ have the following important properties:

Transverse $$\nabla\cdot\mathbf{A}_k(\mathbf{r})=0 \tag{14a}$$

Orthonormal $$\int(d\mathbf{r})\mathbf{A}_j^*(\mathbf{r})\cdot\mathbf{A}_k(\mathbf{r})=\delta_{jk} \tag{14b}$$

Complete $$\sum_k\mathbf{A}_k(\mathbf{r})\mathbf{A}_k^*(\mathbf{r}')=\delta_\perp(\mathbf{r}-\mathbf{r}') \tag{14c}$$

The same statements hold for the $\mathbf{B}_k(\mathbf{r})$s as well. The property in Eq. (14*a*) states the radiation-gauge condition. The integration in Eq. (14*b*) covers the entire volume bounded by the conducting surfaces just mentioned; the eigenvalue equation Eq. (11) holds inside this volume, the so-called quantization volume. In the completeness relation in Eq. (14*c*), both positions $\mathbf{r}$ and $\mathbf{r}'$ are inside the quantization volume, and $\delta_\perp$ is the transverse delta function, a dyadic that is explicitly given by

$$\delta_\perp(\mathbf{r})=\int\frac{(d\mathbf{k})}{(2\pi)^3}\exp(i\mathbf{k}\cdot\mathbf{r})\left(1-\frac{\mathbf{kk}}{k^2}\right) \tag{15}$$

where 1 is the unit dyadic and $k=\sqrt{\mathbf{k}\cdot\mathbf{k}}$ is the length of the wave vector $\mathbf{k}$ integrated over. The transverse character of $\delta_\perp(\mathbf{r})$ ensures the consistency of the properties in Eqs. (14*a*) and (14*c*).

The time dependence of $\mathbf{E}_\perp(\mathbf{r},t)$ and $\mathbf{B}(\mathbf{r},t)$ stems from the ladder operators $a_k(t)$ and $a_k(t)$, which obey the bosonic equal-time commutation relations

$$[a_j,a_k]=0\qquad [a_j,a_k^\dagger]=\delta_{jk}\qquad [a_j^\dagger,a_k^\dagger]=0 \tag{16}$$

The photon number operator

$$N=\sum_k a_k^\dagger a_k \tag{17}$$

has eigenvalues $N'=0, 1, 2, \ldots$; its eigenstates with $N'=1$ are the one-photon states, those with $N'=2$ are the two-photon states, and so on. The unique eigenstate with $N'=0$ is the photon vacuum.

We denote its ket by $|\mathbf{vac}\rangle$. It is, of course, the joint eigenstate of all *annihilation operators* a_k with eigenvalue zero:

$$a_k|\mathbf{vac}\rangle = 0 \qquad \text{for all } k \tag{18}$$

Application of the *creation operator* $a_k^\dagger$ to $|\mathbf{vac}\rangle$ yields a state with one photon in the kth mode:

$$a_k^\dagger|\mathbf{vac}\rangle = \{\text{state with 1 photon of the type } k\} \tag{19}$$

More generally, the ket of a pure one-photon state is of the form

$$|\{\psi\}_1\rangle = \sum_k \psi_k a_k^\dagger|\mathbf{vac}\rangle \qquad \text{with} \qquad \sum_k |\psi_k|^2 = 1 \tag{20}$$

where $|\psi_k|^2$ is the probability for finding the photon in the kth mode. Similarly, the kets of pure two-photon states have the structure

$$|\{\psi\}_2\rangle = \frac{1}{\sqrt{2}}\sum_{j,k}\psi_{jk}a_j^\dagger a_k^\dagger|\mathbf{vac}\rangle \qquad \text{with} \qquad \psi_{jk} = \psi_{kj} \qquad \text{and} \qquad \sum_{j,k}|\psi_{jk}|^2 = 1 \tag{21}$$

and analogous expressions apply to pure states with 3, 4, 5, . . . photons.

Einstein's light quanta are one-photon states of a particular kind. In a manner of speaking, they are localized lumps of electromagnetic energy. In technical terms this means that the energy density

$$\begin{aligned} U_{1\text{ph}}(\mathbf{r},t) &= \left\langle \{\psi\}_1 \left| : \left[\mathbf{E}^2/(2\varepsilon_0) + \left(\frac{\mu_0}{2}\right)\mathbf{B}^2 \right] : \right| \{\psi\}_1 \right\rangle \\ &= \frac{h}{2}\sum_{j,k}\psi_j^*\psi_k\sqrt{\nu_j\nu_k}\,(\mathbf{A}_k^*\cdot\mathbf{A}_j + \mathbf{B}_k^*\cdot\mathbf{B}_j) \end{aligned} \tag{22}$$

is essentially nonzero in a relatively small spatial region only. The time dependence is carried by the probability amplitudes ψ_k, the spatial dependence by the mode functions $\mathbf{A}_k$ and $\mathbf{B}_k$. An arbitrarily sharp localization is not possible, but it is also not needed. The pair of colons :: symbolize the injunction to order the operator in between in the *normal* way: all creation operators $a_k^\dagger$ to the left of all annihilation operators a_k. This normal ordering is an elementary feature of renormalized QED.

At high frequencies, or when the quantization volume is unbounded, the eigenvalues of $-\nabla^2$ in Eq. (11) are so dense that the summations in Eqs. (10), (12), and (14*b*) are effectively integrations, and the Kronecker delta symbol in Eq. (14*b*) is a Dirac delta function. Under these circumstances, it is often natural to choose plane waves

$$\mathbf{A}_k(\mathbf{r}) \sim \mathbf{e}_k \exp\left(i\frac{2\pi\nu_k}{c}\mathbf{n}_k\cdot\mathbf{r}\right) \qquad \mathbf{B}_k(\mathbf{r}) \sim \mathbf{n}_k\times\mathbf{e}_k\exp\left(i\frac{2\pi\nu_k}{c}\mathbf{n}_k\cdot\mathbf{r}\right) \tag{23}$$

for the mode functions. The unit vector $\mathbf{e}_k$ that specifies the polarization is orthogonal to the unit vector $\mathbf{n}_k$ that specifies the direction of propagation.

With

$$\psi_k(t) \sim \exp(-i2\pi\nu_k t) \tag{24}$$

in Eq. (22), one then meets exponential factors of the form

$$\exp\left[i\frac{2\pi\nu_k}{c}(\mathbf{n}_k\cdot\mathbf{r} - ct)\right]$$

As a consequence, an einsteinian light quantum propagates without dispersion, which is the anticipated behavior.

The one-photon energy density in Eq. (22) illustrates the general feature that quantum-mechanical probabilities (the ψ_ks) with their interference properties appear together with the classical interference patterns of superposed mode functions [the $\mathbf{A}_k(\mathbf{r})$s and $\mathbf{B}_k(\mathbf{r})$s]. In other words, interference phenomena of two kinds are present in QED: (1) the classical interference of electromagnetic fields in the three-dimensional $\mathbf{r}$ space, and (2) the quantum interference of alternatives in the so-called Fock space; that is, the Hilbert space spanned by the photon vacuum $|\mathbf{vac}\rangle$, the one-photon states $|\{\psi\}_1\rangle$, the two-photon states $|\{\psi\}_2\rangle$, and all multiphoton states.

In the early days of QED, this coexistence of classical interferences and quantum interferences was a research topic, to which Fermi's paper of 1929 "Sulla teoria quantistica delle frange di interferenza" is a timeless contribution.[45] He demonstrated, at the example of Lippmann fringes, a very general property of single-photon interference patterns: the photon-counting rates, as determined from quantum-mechanical probabilities, are proportional to the corresponding classical intensities.

Electromagnetic radiation is easily emitted and absorbed by antennas, processes that change the number of photons. Accordingly, the number of photons is not a conserved quantity, and therefore states of different photon numbers can be superposed. Particularly important are the *coherent states*

$$|\{\alpha\}_c\rangle = \exp\left(-\frac{1}{2}\sum_k |\alpha_k|^2 + \sum_k \alpha_k a_k^\dagger\right)|\mathbf{vac}\rangle \tag{25}$$

that are characterized by a set $\{\alpha\}_c$ of complex amplitudes α_k. As revealed in Glauber's 1963 papers,[46–48] they play a central role in the coherence theory of light.

Since the coherent states are common eigenstates of the annihilation operators

$$a_k|\{\alpha\}_c\rangle = |\{\alpha\}_c\rangle\alpha_k \tag{26}$$

the expectation values of the electric and magnetic field operators of Eqs. (10) and (12)

$$\begin{aligned}\langle\{\alpha(t)\}_c|\mathbf{E}_\perp(\mathbf{r},t)|\{\alpha(t)\}_c\rangle &= \sum_k \sqrt{\frac{h\nu_k}{(2\varepsilon_0)}}[\alpha_k(t)\mathbf{A}_k(\mathbf{r}) + \alpha_k^*(t)\mathbf{A}_k^*(\mathbf{r})] \\ \langle\{\alpha(t)\}_c|\mathbf{B}_\perp(\mathbf{r},t)|\{\alpha(t)\}_c\rangle &= \sum_k \sqrt{\frac{\mu_0 h\nu_k}{2}}[-i\alpha_k(t)\mathbf{B}_k(\mathbf{r}) + i\alpha_k^*(t)\mathbf{B}_k^*(\mathbf{r})]\end{aligned} \tag{27}$$

have the appearance of classical Maxwell fields. In more general terms, if the statistical operator ϱ_{ph} of the photonic degrees of freedom—in other words, the statistical operator of the radiation field—is a mixture of (projectors to) coherent states

$$\varrho_{\text{ph}} = \sum_{\{\alpha\}_c} |\{\alpha\}_c\rangle\, w(\{\alpha\}_c)\langle\{\alpha\}_c| \tag{28}$$

with

$$w(\{\alpha\}_c) \geq 0 \quad \text{and} \quad \sum_{\{\alpha\}_c} w(\{\alpha\}_c) = 1 \tag{29}$$

then the electromagnetic field described by ϱ_{ph} is very similar to a classical Maxwell field. Turned around, this says that whenever it is impossible to write a given ϱ_{ph} in the form of Eq. (28), then some statistical properties of the radiation are decidedly nonclassical.

During the 20-year period from Dirac's paper of 1927 to the Shelter Island conference in 1947, QED remained in a preliminary state that allowed various studies—the most important ones included the Weisskopf-Wigner treatment of spontaneous emission[49] and Weisskopf's discovery that the self-energy of the photon is logarithmically divergent[50]—although the not-yet-understood divergences

were very troublesome. The measurement by Lamb and Retherford[51] of what is now universally known as the *Lamb shift*, first reported at the Shelter Island conference, was the crucial experimental fact that triggered the rapid development of renor-malized QED by Schwinger, Feynman, and others.

Theoretical calculations of the Lamb shift rely heavily on the quantum properties of the electromagnetic field, and their marvelous agreement with the experimental data proves convincingly that these quantum properties are a physical reality. In other words, photons exist. The same remark applies to the theoretical and experimental values of the anomalous magnetic moment of the electron, one of the early triumphs of Schwinger's renormalized QED,[52] which finally explained an anomaly in the spectra of hydrogen and deuterium that Pasternack had observed in 1938[53] and a discrepancy in the measurements by Millman and Kusch[54] of nuclear magnetic moments.

Photon-Photon Correlations

Interferometers that exploit not the spatial intensity variations (or, equivalently, the photon-detection probabilities) but correlations between intensities at spatially separated positions became important tools in astronomy and spectroscopy after the discovery of the Hanbury-Brown-Twiss (HB&T) effect in 1954.[55–57] A textbook account of its classical theory is given in Sec. 4.3 of Ref. 58.

In more recent years, the availability of single-photon detectors made it possible to study the HB&T effect at the two-photon level. The essentials are depicted in Fig. 2. Two light quanta are incident on a half-transparent mirror from different directions, such that they arrive simultaneously. If their frequency contents are the same, it is fundamentally impossible to tell if an outgoing light quantum was reflected or transmitted. This indistinguishability of the two light quanta is of decisive importance in the situation where one is in each output channel. The two cases *both reflected* and *both transmitted* are then indistinguishable and, according to the laws of quantum mechanics, the corresponding probability amplitudes must be added.

Now, denoting the probability amplitudes for single-photon reflection and transmission by ρ and τ, respectively, the probability for one light quantum in each output port is given by

$$|\rho^2+\tau^2|^2=\left|\left(\frac{1}{\sqrt{2}}\right)^2+\left(\frac{i}{\sqrt{2}}\right)^2\right|^2=0 \tag{30}$$

where we make use of $\rho=1/\sqrt{2}$ and $\tau=i/\sqrt{2}$, which are the values appropriate for a symmetric half-transparent mirror. Thus, the situation of one light quantum in each output port does not occur. Behind the half-transparent mirror, one always finds both light quanta in the same output port.

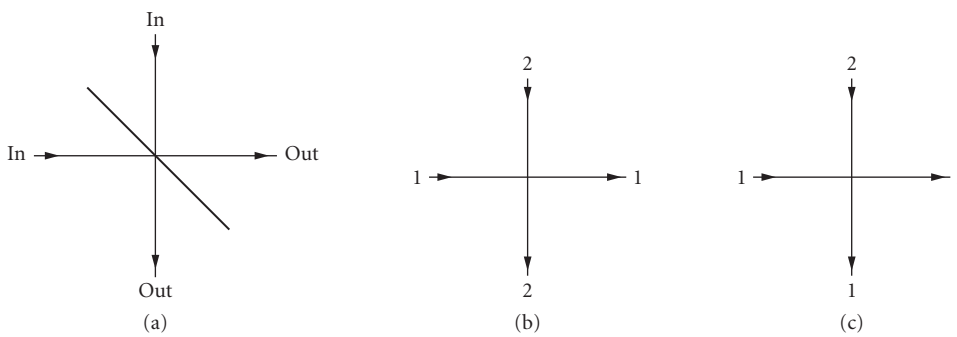

FIGURE 2 Essentials of the Hanbury-Brown–Twiss effect at the two-photon level. (*a*) Two light quanta are simultaneously incident at a symmetric half-transparent mirror. To obtain one quantum in each output port, the quanta must be either both transmitted (*b*) or both reflected (*c*). The probability amplitude for (*b*) is $(1/\sqrt{2})^2=1/2$, that for (*c*) is $(i/\sqrt{2})^2=-1/2$. If the two cases are indistinguishable, the total amplitude is $1/2-1/2=0$.

If the light quanta arrived at very different times, rather than simultaneously, they would be distinguishable and one would have to add probabilities instead of probability amplitudes, so that

$$|\rho^2|^2 + |\tau^2|^2 = \frac{1}{2} \tag{31}$$

would replace Eq. (30). Clearly, there are intermediate stages at which the temporal separation is a fraction of the temporal coherence length and the two quanta are neither fully distinguishable nor utterly indistinguishable. The probability for one light quantum in each output port is then a function of the separation, a function that vanishes when the separation does.

Experiments that test these considerations[59] employ correlated photon pairs produced by a process known as *parametric downconversion*. Roughly speaking, inside a crystal that has no inversion symmetry a high-frequency photon is absorbed and two lower-frequency photons are emitted, whereby the conservation of energy and momentum imposes geometrical restrictions on the possible propagation directions of the three photons involved. Downconversion sources with a high luminosity are available.[60,61]

The HB&T effect of Fig. 2 as well as closely related phenomena are crucial in many experiments in which entangled photons are a central ingredient. In particular, the recent realizations[62,63] of schemes for quantum teleportation[64] and the experiment[65] that demonstrated the practical feasibility of quantum-dense coding[66] are worth mentioning here.

None of these exciting developments could be understood without the quantum properties of radiation. Since the photon concept, in the sense of the discussion of Eqs. (10), (12), (19), (20), and so on is an immediate consequence of these quantum properties, the existence of photons is an established experimental fact beyond reasonable doubt.

23.4 QUANTUM THEORY OF THE LASER

The quantum theory of laser radiation is a problem in nonequilibrium statistical mechanics. There are several alternative, but ultimately equivalent, approaches to the characterization of the field inside the resonator. As is customary in the Scully-Lamb quantum theory, we describe the state of the laser field by a density operator.[67,68] In this section our main focus is on the review of the equation of motion, the so-called master equation, for this density operator as it emerges from an underlying physical model, with statistical considerations and some simplifying assumptions. The alternative procedure based on the quantum theory of noise sources introduced in Refs. 69 and 70 and summarized in Refs. 71 to 74 will also be briefly reviewed at the end of the section. For a recent, more detailed overview of the quantum Langevin point of view, we refer the reader to Ref. 75.

In general, a laser model should be based on the interaction of multimode fields with multilevel atoms as the active medium, and a detailed consideration of all possible processes among all the levels involved should be given. Decay channels and decay rates, in particular, play a crucial role in determining the threshold inversion and, thus, the necessary pumping rates. Of course, the pumping mechanisms themselves can be quite complicated. It is well established that a closed two-level model cannot exhibit inversion and, hence, lasing. In order to achieve inversion three- and four-level pumping schemes are employed routinely. On the other hand, to illustrate the essential quantum features a single mode field can serve as paradigm. The single-mode laser field inside the resonator interacts with one particular transition of the multilevel system—the lasing transition—and the role of the entire complicated level structure is to establish inversion on this transition—that is, to put more atoms in the upper level than there are in the lower one. If one is not interested in the details of how the inversion builds up, it is possible to adopt a much simpler approach than the consideration of a multilevel-multimode system. In order to understand the quantum features of the single-mode field it is sufficient to focus only on the two levels of the lasing transition and their interaction with the laser field. In this approach, the effect of pumping, decay, and so on in the multilevel structure is simply replaced by an initial condition; it is assumed that the atom is in its upper state immediately before the interaction with the laser mode begins. Since here we are primarily interested

in the quantum signatures of the laser field and not in the largely classical aspects of cavity design, pumping mechanisms, and so on, we shall follow this simpler route from the beginning. The model that accounts for the resonant interaction of a two-level atom with a single quantized mode in a cavity was introduced by Jaynes and Cummings.[76]

We shall make an attempt to present the material in a tutorial way. We first derive an expression for the change of the field density operator due to the interaction with a single two-level atom, initially in its upper state, using the Jaynes-Cummings model. This expression will serve as the seed for both the laser and micromaser theories. We next briefly review how to account for cavity losses by using standard methods for modeling the linear dissipation loss of the cavity field due to mirror transmission. Then we show that with some additional assumptions the single-atom-single-mode approach can be used directly to derive what has become known as the Scully-Lamb master equation for the more traditional case of the laser and the micromaser. The additional assumptions include the Markov approximation or, equivalently, the existence of very different time scales for the atomic and field dynamics so that adiabatic elimination of the atoms and introduction of coarse-grained time evolution for the field become possible. The main difference between the laser and micromaser theories is that the interaction time of the active atoms with the field is governed by the lifetime of the atoms in the laser and by the transit time of the atoms through the cavity in the micromaser. In the laser case, the atoms decay out of the lasing levels into some far-removed other levels, and they are available for the lasing transition during their lifetime on the average. In the micromaser case, the transit time is approximately the same for all atoms in a monoenergetic pumping beam. Thus, the laser involves an extra averaging over the random interaction times. If we model the random interaction times by a Poisson distribution and average the change of the field density operator that is due to a single atom—the kick—over the distribution of the interaction times, we obtain the master equation of a laser from that of the micromaser. Historically, of course, the development was just the opposite: the master equation was derived in the context of the laser much earlier. However, it is instructive to see how the individual Rabi oscillations of single nondecaying atoms with a fixed interaction time, as in the micromaser, give rise to the saturating, nonoscillatory collective behavior of an ensemble of atoms, as in the laser, upon averaging over the interaction times. As applications of this fully quantized treatment we study the photon statistics, the linewidth, and spectral properties. Finally, we briefly discuss other approaches to the quantum theory of the laser.

Time Evolution of the Field in the Jaynes-Cummings Model

We shall consider the interaction of a single two-level atom with a single quantized mode of a resonator using the rotating-wave approximation (for a recent review of the Jaynes-Cummings model see Ref. 77). The arrangement is shown in Fig. 3.

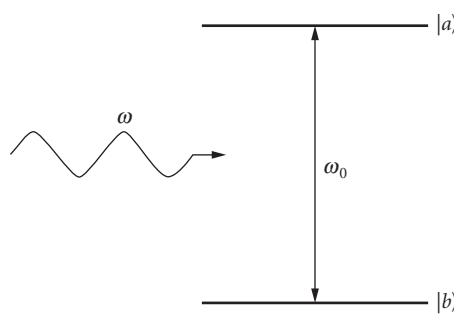

FIGURE 3 Scheme of a two-level atom interacting with a single mode quantized field. The text focuses on the resonant case, $\omega = \omega_0$.

The hamiltonian for this system is given by

$$\mathcal{H} = \mathcal{H}_0 + \mathcal{H}_1 \tag{32}$$

where

$$\mathcal{H}_0 = \frac{1}{2}\hbar\omega_0\sigma_z + \hbar\omega_0 a^\dagger a \tag{33}$$

and

$$\mathcal{H}_1 = \hbar g(\sigma_+ a + a^\dagger \sigma_-) \tag{34}$$

Here a and $a^\dagger$ are the annihilation and creation operators for the mode. The upper level of the lasing transition is denoted by $|a\rangle$ and the lower level by $|b\rangle$. The atomic lowering and raising operators are expressed in terms of the state vectors as $\sigma_- = (\sigma_+)^\dagger = |b\rangle\langle a|$ and the population operator as $\sigma_z = |a\rangle\langle a| - |b\rangle\langle b|$ ω_0 is the frequency of the $|a\rangle - |b\rangle$ transition. For simplicity we assume perfect resonance with the mode. Finally, g is the coupling constant between the atom and the mode. In terms of atomic and field quantities it is given by $g = p\sqrt{\omega_0/2\hbar\varepsilon_0 v}$ where p is the transition dipole moment and v the quantization volume (the volume of the active medium, in our case). Again, for simplicity, p is assumed to be real.

In the interaction picture with respect to $\mathcal{H}_0$, the interaction hamiltonian becomes

$$\mathcal{V} = \exp\left(\frac{i\mathcal{H}_0 t}{\hbar}\right)\mathcal{H}_1 \exp\left(-\frac{i\mathcal{H}_0 t}{\hbar}\right) = \hbar g\left(\sigma_+ a + a^\dagger \sigma_-\right) \equiv \mathcal{H}_1 \tag{35}$$

since $\mathcal{H}_0$ and $\mathcal{H}_1$ commute.

In the two-dimensional Hilbert space spanned by the state vectors $|a\rangle$ and $|b\rangle$ the interaction hamiltonian can be written as

$$\mathcal{H}_1 = \hbar g\begin{pmatrix} 0 & a \\ a^\dagger & 0 \end{pmatrix} \tag{36}$$

The time evolution operator for the coupled atom-field system satisfies the equation of motion in this picture

$$\frac{i\hbar dU}{dt} = \mathcal{V}U \tag{37}$$

and since $\mathcal{H}_1$ is time independent the solution is formally

$$U(\tau) = \exp\left(-\frac{i}{h}\mathcal{V}\tau\right) \tag{38}$$

Using the properties of the σ_- and σ_+ matrices, it is easy to show that $U(\tau)$ can be written in the preceding 2×2 matrix representation as

$$U(\tau) = \begin{pmatrix} \cos\left(g\tau\sqrt{aa^\dagger}\right) & -i\dfrac{\sin\left(g\tau\sqrt{aa^\dagger}\right)}{\sqrt{aa^\dagger}}a \\ -ia^\dagger\dfrac{\sin\left(g\tau\sqrt{aa^\dagger}\right)}{\sqrt{aa^\dagger}} & \cos\left(g\tau\sqrt{a^\dagger a}\right) \end{pmatrix} \tag{39}$$

Let us now assume that initially, at t_0, the atom is in its upper state given by the atomic density operator $\varrho_{at}(t_0)=|a\rangle\langle a|$ and the field is in an arbitrary state which, in general, can be described by the density operator $\varrho(t_0)$, so that the joint atom-field system is characterized by the initial density operator $\varrho_{af}(t_0)=\varrho_{at}(t_0)\otimes\varrho(t_0)$. After the interaction, $\varrho_{af}(t_0+\tau)=U(\tau)\varrho_{af}(t_0)U(\tau)^{-1}$. Our main interest here is in the evolution of the field density operator. This we obtain if we trace the atom-field density operator over the atomic states, yielding

$$\begin{aligned}\varrho(t_0+\tau)&=\mathrm{Tr}_{\mathrm{atom}}[\varrho_{af}(t+\tau)]\\&=\cos(g\tau\sqrt{aa^\dagger})\varrho(t_0)\cos(g\tau\sqrt{aa^\dagger})+a^\dagger\frac{\sin(g\tau\sqrt{aa^\dagger})}{\sqrt{aa^\dagger}}\varrho(t_0)\frac{\sin(g\tau\sqrt{aa^\dagger})}{\sqrt{aa^\dagger}}a\\&\equiv M(\tau)\varrho(t_0)\end{aligned}\tag{40}$$

Here in the last step we just introduced the superoperator M, which describes the effect of a single inverted atom on the field and is a key ingredient of laser and micromaser theory. The matrix elements in photon number representation take the form

$$(M(\tau)\varrho)_{nn'}=A_{nn'}(\tau)\varrho_{nn'}+B_{n-1n'-1}(\tau)\varrho_{n-1n'-1}\tag{41}$$

where the coefficients are given by

$$A_{nn'}(\tau)=\cos(g\tau\sqrt{n+1})\cos(g\tau\sqrt{n'+1})\tag{42}$$

$$B_{nn'}(\tau)=\sin(g\tau\sqrt{n+1})\sin(g\tau\sqrt{n'+1})\tag{43}$$

For later purposes, we also introduce the change in the state of the field due to the interaction with a single inverted atom as

$$\varrho(t_0+\tau)-\varrho(t_0)=M(\tau)\varrho(t_0)-\varrho(t_0)=(M-1)\varrho(t_0)\equiv K\varrho(t_0)\tag{44}$$

The operator K, sometimes called the *kick operator*, contains all the information we will need to build the quantum theory of the single-mode laser and micromaser. In matrix representation, $[K(\tau)\varrho]_{nn'}=[A_{nn'}(\tau)-\delta_{nn'}]\varrho_{nn'}+B_{n-1n'-1}(\tau)\varrho_{n-1n'-1}$.

For more elaborate systems (multimode lasers driven by multilevel atoms, for example) one cannot give M in such a simple analytical form, but the principle remains always the same. One should find the superoperator M or, equivalently, the kick operator $K=M-1$ which gives the action of a single (possibly multilevel) atom on the (possibly multimode) field from the general expression $\varrho(t_0+\tau)=\mathrm{Tr}_{\mathrm{atom}}[U_{af}(\tau)\varrho_{at}(t_0)\otimes\varrho(t_0)U_{af}(\tau)^{-1}]\equiv M(\tau)\varrho(t_0)$. In order to determine the full time-evolution operator $U_{af}(\tau)$ of the coupled atom-field system, however, one usually needs to resort to approximation methods, such as perturbation theory, in the more complicated multilevel-multimode cases.

Derivation of the Scully-Lamb Master Equation

In 1954, Gordon, Zeiger, and Townes showed that coherent electromagnetic radiation can be generated in the radio frequency range by the maser (acronym for *microwave amplification by stimulated emission of radiation*).[78] The first maser action was observed in a beam of ammonia.[79] The maser principle was extended to the optical domain by Schawlow and Townes,[80] and also by Prokhorov

and Basov,[81] thus obtaining a laser (acronym for *light amplification by stimulated emission of radiation*). A laser consists of a large ensemble of inverted atoms interacting resonantly with the electromagnetic field inside a cavity. The cavity selects only a specific set of modes corresponding to a discrete set of eigenfrequencies. The active atoms—that is, the ones that are pumped to the upper level of the laser transition—are in resonance with one of the eigenfrequencies of the cavity in the case of the single-mode laser and with a finite set of frequencies in the case of the multimode laser. As discussed in the introduction to this section, for the discussion of the essential quantum features of the radiation field of a laser it is sufficient to confine our treatment to the single-mode case, and that is what we will do for the remainder of this section. A resonant electromagnetic field gives rise to stimulated emission, and the atoms thereby transfer their energy to the radiation field. The emitted radiation is still at resonance. If the upper level is sufficiently populated, this radiation gives rise to further transitions in other atoms. In this way, all the excitation energy of the atoms is transferred to the single mode of the radiation field.

The first pulsed laser operation was demonstrated by Maiman in ruby.[82] The first continuous wave (CW) laser, a He-Ne gas laser, was built by Javan et al.[83] Since then a large variety of systems have been demonstrated to exhibit lasing action. Coherent radiation has been generated this way over a frequency domain ranging from infrared to soft X rays. These include dye lasers, chemical lasers, solid-state lasers, and semiconductor lasers.

Many of the laser properties can be understood on the basis of a semiclassical theory. In such a theory the radiation field is treated classically, but the active medium is given a full quantum-mechanical treatment. Such a theory can readily explain threshold and saturation, transient dynamics, and general dependence on the external parameters (pumping and losses). It is not our aim here to give an account of the semiclassical theory; therefore, we just refer the reader to the ever instructive and wonderfully written seminal paper by Lamb[84] and a more extended version in Ref. 67. Although quantum effects play only a minor role in usual practical laser applications because of the large mean photon numbers, they are essential for the understanding of the properties of micromasers, in which excited two-level atoms interact one after the other with a single mode of the radiation field.[85] Nevertheless, the quantum properties of the laser field are of fundamental interest as well. They have been thoroughly investigated theoretically with respect to the photon statistics and the spectrum of the laser. In particular, the quantum limitation of the laser linewidth caused by the inevitably noisy contribution of spontaneous emission has attracted much attention. It gives rise to the so-called Schawlow-Townes linewidth, which is inversely proportional to the laser intensity (see Ref. 80). Because of the importance of stable coherent signals for various high-precision measurements, the problem of the intrinsic quantum-limited linewidth has gained renewed interest recently, and the investigations have been extended to cover bad-cavity lasers and several more exotic systems. In this review, however, we shall restrict ourselves to good-cavity lasers in which the cavity damping time is long compared to all other relevant time scales, and present a fully quantized theory of the most fundamental features.

Cavity Losses To account for the decay of the cavity field through the output mirror of the cavity, we simply borrow the corresponding result from reservoir theory. Its usage has become fairly standard in laser physics and quantum optics (see, for example, Refs. 67 and 68), and here we just quote the general expression without actually deriving it.

$$\left(\frac{d\varrho}{dt}\right)_{\text{loss}} = \mathcal{L}\varrho \equiv -\frac{\kappa}{2} n_{\text{th}} (aa^\dagger \varrho + \varrho aa^\dagger - 2a^\dagger \varrho a) - \frac{\kappa}{2}(n_{\text{th}} + 1)(a^\dagger a\varrho + \varrho a^\dagger a - 2a\varrho a^\dagger) \tag{45}$$

This equation refers to a loss reservoir which is in thermal equilibrium at temperature T, with n_{th} being the mean number of thermal photons $n_{\text{th}} = [\exp(\hbar\omega_0 / kT) - 1]^{-1}$, and κ is the cavity damping rate. For the laser case, it is sufficient to take the limiting case of a zero temperature reservoir since $\hbar\omega_0 \gg kT$ and n_{th} is exponentially small. We obtain this limit by substituting $n_{\text{th}} = 0$ into Eq. (45). For the description of most micromaser experiments, however, we need the finite temperature version, since even at very low temperatures the thermal photon number is comparable to the total number of photons in the cavity.

QUANTUM THEORY OF THE LASER

The Laser Master Equation After introducing the loss part of the master equation, we now turn our attention to the part that stems from the interaction with the gain reservoir. The gain reservoir is modeled by an ensemble of initially excited two-level atoms allowed to interact with the single-mode cavity field. A central role in our subsequent discussions will be played by the so-called kick operator, $K = M - 1$, describing the change of the field density operator due to the interaction with a single atom. This quantity was introduced in Eq. (44). While in the micromaser case the effect of each of the atoms can be represented by the same kick operator, since in a monoenergetic pumping beam each atom has the same interaction time with the cavity field, this is no longer the case for a laser. In a typical CW gas laser, such as the He-Ne laser, atoms are excited to the upper level of the lasing transition at random times and, more important, they can also interact with the field for a random length of time. The interaction time thus becomes a random variable. Since at any given time the number of atoms is large (about 10^6 to 10^7 active atoms in the lasing volume of a CW He-Ne laser), it is a legitimate approach to describe their effect on the field by an average kick operator. We can arrive at the interaction-time-averaged master equation quickly if we take the average of Eq. (44) with respect to the interaction time τ:

$$(M-1)\varrho(t)=\int_0^\infty d\tau P(\tau)(M(\tau)-1)\varrho(t) \tag{46}$$

where the distribution function for the interaction time $P(\tau)$ is defined as

$$P(\tau)=\gamma e^{-\gamma\tau} \tag{47}$$

This distribution function corresponds to the exponential decay law. Individual atoms can decay from the lasing levels at completely random times, but for an ensemble of atoms the probability of finding an initially excited atom still in the lasing levels in the time interval $(\tau, \tau+d\tau)$ is given by Eq. (47). With increasing τ it is increasingly likely that the atoms have decayed outside the lasing transition. Also note that our model corresponds to an open system: the atoms decay to other non-lasing levels both from the upper state $|a\rangle$ and the lower state $|b\rangle$, and, in addition, we assume that decay rate γ is the same for both levels, as indicated in Fig. 4.

Obviously, these restrictions can be relaxed and, indeed, there are various more general models available. For example, the upper level $|a\rangle$ can have two decay channels. It can decay to the lower level $|b\rangle$ and to levels outside the lasing transition. Or, in some of the most efficient lasing schemes, the lower level decays much faster than the upper one, $\gamma_b \gg \gamma_a$. In these schemes virtually no population builds up in the lower level; hence, saturation of the lasing transition occurs at much higher

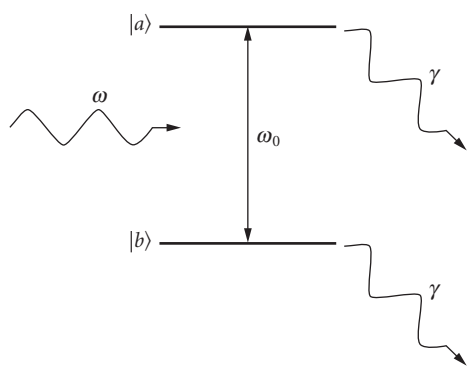

FIGURE 4 Scheme of a two-level atom, with atomic decay permitted, interacting with a single-mode quantized field.

intensities than in lasers with equal decay rates for both levels. These generalizations, however, are easily accounted for (see Ref. 67) and it is not our concern here to provide the most general treatment possible. Instead, we want to focus on the essential quantum features of the laser field and employ the simple two-level model with equal decay rates for both.

The formal averaging in Eq. (46) can be performed most easily if we transform to a particular representation of the density matrix. For our purposes, the photon number representation suffices, although other options are readily available and some of them will be summarized briefly at the end of this section. Taking the n, n' elements of Eq. (46) and using Eqs. (42) and (43), the averaging yields

$$[(M-1)\varrho]_{nn'} = -\frac{\chi(n+1+n'+1)+\chi^2(n-n')^2}{1+2\chi(n+1+n'+1)+\chi^2(n-n')^2}\varrho_{nn'} + \frac{2\chi\sqrt{nn'}}{1+2\chi(n+n')+\chi^2(n-n')^2}\varrho_{n-1n'-1} \tag{48}$$

where the notation $\chi = g^2/\gamma^2$ is introduced. Finally, taking into account cavity losses $(\mathcal{L}\varrho)_{nn'}$ from Eq. (45), with $n_{\text{th}} = 0$, we obtain the following master equation for our quantum-mechanical laser model:

$$\dot{\varrho}_{nn'} = -\frac{\mathcal{N}'_{nn'}\mathcal{A}}{1+\mathcal{N}_{nn'}\mathcal{B}/\mathcal{A}}\varrho_{nn'} + \frac{\sqrt{nn'\mathcal{A}}}{1+\mathcal{N}_{n-1n'-1}\mathcal{B}/\mathcal{A}}\varrho_{n-1n'-1} - \frac{\kappa}{2}(n+n')\varrho_{nn'} + \kappa\sqrt{(n+1)(n'+1)}\varrho_{n+1n'+1} \tag{49}$$

Here we introduced the original notations of the Scully-Lamb theory—the linear gain coefficient:

$$\mathcal{A} = 2r\chi \tag{50}$$

the self-saturation coefficient:

$$\mathcal{B} = 4\chi\mathcal{A} \tag{51}$$

and the dimensionless factors:

$$\mathcal{N}' = \frac{1}{2}(n+1+n'+1) + \frac{(n-n')^2\mathcal{B}}{8\mathcal{A}} \tag{52}$$

and

$$\mathcal{N} = \frac{1}{2}(n+1+n'+1) + \frac{(n-n')^2\mathcal{B}}{16\mathcal{A}} \tag{53}$$

Equation (49) is the Scully-Lamb master equation, which is the central equation of the quantum theory of the laser. Along with the notations introduced in Eqs. (50) to (53), it constitutes the main result of this section and serves as the starting point for our treatment of the quantum features of the laser. Among the specific problems we shall consider are the photon statistics, which is the physical information contained in the diagonal elements, and the spectrum, which is the physical information contained in the off-diagonal elements of the field density matrix.

The Micromaser Master Equation The development of the single-atom maser or micro-maser plays a particularly important role in cavity quantum electrodynamics because it realizes one of the most fundamental models, the Jaynes-Cummings hamiltonian. The experimental situation[86] is very close to the idealized case of a single two-level atom interacting with a single-mode quantized field, as previously discussed, and allows a detailed study of fundamental quantum effects in the atom-field interaction.

In the micromaser, a stream of two-level atoms is injected into a superconducting microwave cavity of very high quality Q. The injection rate r is low enough to ensure that at most only one atom is present inside the cavity at any given time and that most of the time the cavity is empty. The decay time of the high-Q cavity field is very long compared to both the interaction time τ, which is set by the transit time of atoms through the cavity, and the inverse of the single-photon Rabi frequency g^{-1}. In typical experimental situations, however, $g\tau \simeq 1$. Therefore, a field is built up in the cavity provided the interval between atomic injections does not significantly exceed the cavity decay time. Sustained oscillation is possible with less than one atom on the average in the cavity.

In addition to the progress in constructing superconducting cavities, advances in the selective preparation of highly excited hydrogenlike atomic states, called *Rydberg states*, have made possible the realization of the micromaser. In Rydberg atoms the probability of induced transitions between adjacent states is very large, and the atoms may undergo several Rabi cycles— that is, several periodic energy exchanges between the atom and the cavity field may take place in the high-Q cavity. The lifetime of Rydberg states for spontaneous emission decay is also very long, and atomic decay can be neglected during the transit time in the cavity.

Here we set out to derive a master equation for the micromaser. For this, we consider a single-mode resonator into which two-level atoms are injected in their upper states. Due to the different time scales, the effect of cavity damping can be neglected during the interaction. Then the effect of a single atom on the field density operator, injected at t_i and interacting with the field for a time τ, is given by Eq. (44) with t_0 replaced by t_i. If several atoms are injected during a time interval Δt which is still short on the time scale governed by the cavity decay time κ^{-1} but long on the time scale of the interaction time τ, then the cumulative effect on the field is simply the sum of changes

$$\Delta\boldsymbol{\varrho} = \sum_{t \le t_i \le t+\Delta t} (M(\tau)-1)\boldsymbol{\varrho}(t_i) = r\int_{t}^{t+\Delta t} (M(\tau)-1)\boldsymbol{\varrho}(t_i)dt_i \tag{54}$$

where in the last step we turned the sum into an integral by using the injection rate r as the number of excited-state atoms entering the cavity per unit time.

At this point we introduce some of the most important approximations of laser physics, or reservoir theory in general—the so-called Markov or adiabatic approximation and coarse time graining. These approximations are based on the existence of three very different time scales in the problem. First, the interaction time τ for individual atoms is of the order of the inverse single-photon Rabi frequency g^{-1}, and is the shortest of all. In fact, on the time scale set by the other relevant parameters, it appears as a delta-function-like kick to the state of the field with the kick operator K of Eq. (44). The second time scale is set by r^{-1}, the average time separation between atomic injections. It is supposed to be long compared to τ but short compared to the cavity-damping time κ^{-1}. Thus, we have the following hierarchy of timescales: $\tau \ll r^{-1} \ll \kappa^{-1}$. When we turned the sum in Eq. (54) into an integral we already tacitly assumed that there is a time scale on which the injection appears to be quasicontinuous. We now see that it is the time scale set by κ^{-1}. This is the time scale that governs the time evolution of the cavity field. In the evaluation of the integral in Eq. (54) we assume that Δt is an intermediate time interval such that $r^{-1} < \Delta t < \kappa^{-1}$. Then during this interval the state of the field does not change appreciably, and we can replace $\boldsymbol{\varrho}(t_i)$ on the right-hand side of Eq. (54) by $\boldsymbol{\varrho}(t)$. This is the essential step in transforming the integral equation into a differential equation, and it constitutes what is called the *Markov approximation*. It is also called the *adiabatic approximation* since the field changes very slowly (adiabatically) on the time scale set by the atoms. As a result, $\boldsymbol{\varrho}(t)$ can now be taken out of the integral, and the integration in Eq. (54) yields $\Delta\boldsymbol{\varrho} = r\Delta t\big(M-1\big)\boldsymbol{\varrho}(t)$. Dividing both sides by Δt, we obtain

$$\frac{\Delta\boldsymbol{\varrho}}{\Delta t} = r(M(\tau)-1)\boldsymbol{\varrho} \tag{55}$$

The left-hand side is not a true derivative; it only appears to be one on the time scale of the cavity decay time. However, if we are interested in the large-scale dynamics of the field, we can still regard it as a good approximation to a time derivative. It is called the *coarse-grained derivative* and the Eq. (55)

now properly describes the time rate of change of the field due to the interaction with an ensemble of active atoms, the gain reservoir.

Equation (55) gives the time rate of change of the field density operator due to the gain reservoir $(d\varrho/dt)_{\text{gain}}$. To this, we add the time rate of change of the density operator due to the cavity losses by hand. For the parameters of the Garching micromaser experiment, $T = 0.5$ K and $\omega_0/2\pi = 21.5$ GHz, yielding $n_{\text{th}} = 0.15$. The thermal background cannot be neglected since, as we shall see, the steady-state field contains but a few photons. The complete master equation for the micromaser, including both gain and loss, is then simply the sum of Eqs. (55) and (45):

$$\frac{d\varrho}{dt} = \left(\frac{d\varrho}{dt}\right)_{\text{gain}} + \left(\frac{d\varrho}{dt}\right)_{\text{loss}} = r(M(\tau)-1)\varrho + \mathcal{L}\varrho \tag{56}$$

For later purposes, we also give the master equation in matrix representation:

$$\begin{aligned}\frac{d\varrho_{nn'}}{dt} = {} & r[(A_{nn'}(\tau)-1)\varrho_{nn'} + B_{n-1n'-1}(\tau)\varrho_{n-1n'-1}] \\ & -\frac{\kappa}{2}n_{\text{th}}[(n+n'+2)\varrho_{nn'} - 2\sqrt{nn'}\varrho_{n-1n'-1}] \\ & -\frac{\kappa}{2}(n_{\text{th}}+1)[(n+n')\varrho_{nn'} - 2\sqrt{(n+1)(n'+1)}\varrho_{n+1n'+1}]\end{aligned} \tag{57}$$

Here $A_{nn'}(\tau)$ and $B_{nn'}(\tau)$ are given by Eqs. (42) and (43). Equation (57) is identical to the one obtained by more standard methods[87] and employed widely in the context of micromasers. It forms the basis for most studies (with a few notable exceptions, as discussed at the end of this section) on the quantum statistical properties of the micromaser and, naturally, it will be our starting point as well.

Physics on the Main Diagonal: Photon Statistics

To begin to bring to light the physical consequences of the laser and maser master equations, we shall first focus on the diagonal elements of the field density matrix ϱ_{nn}, which give us the photon-number distribution since $\varrho_{nn} = p(n)$ is the probability of finding n photons in the cavity mode. The case of the laser is sufficiently different from that of the micromaser that we shall deal with them separately.

Laser Photon Statistics Taking the diagonal $n = n'$ elements in Eq. (49) and regrouping the terms, we obtain the following equation for the photon-number probabilities:

$$\dot{p}(n) = -\frac{(n+1)\mathcal{A}}{1+(n+1)\mathcal{B}/\mathcal{A}}p(n) + \kappa(n+1)p(n+1) + \frac{n\mathcal{A}}{1+n\mathcal{B}/\mathcal{A}}p(n-1) - \kappa n p(n) \tag{58}$$

Here the overdot stands for the time derivative. Note that diagonal elements are coupled only to diagonal elements. This holds quite generally; Eq. (49) describes coupling along the same diagonal only. For example, elements on the first side diagonal are coupled to other elements on the first side diagonal, and so on, and in general only elements with the same difference $n - n'$ are coupled. The quantity $k = n - n'$ corresponds to elements on the kth side diagonal. Elements on different diagonals are not coupled, which greatly simplifies the solution of laser-related problems.

Before we begin the solution of Eq. (58), we want to give a simple intuitive physical picture of the processes it describes in terms of a probability flow diagram, shown in Fig. 5.

The left-hand side is the rate of change of the probability of finding n photons in the cavity. The right-hand side contains the physical processes that contribute to the change. Each process is

QUANTUM THEORY OF THE LASER

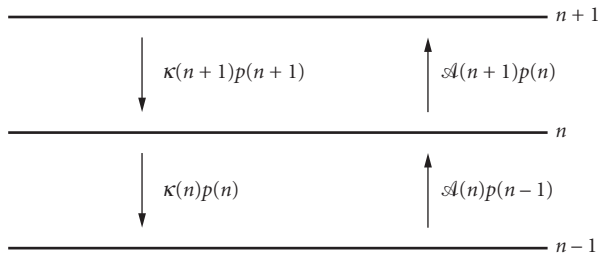

FIGURE 5 Probability flow diagram for the laser.

represented by an arrow in the diagram. The processes are proportional to the probability of the state they are starting from and this will be the starting point of the arrow. The tip of the arrow points to the state the process is leading to. There are two kinds of elementary processes: emission of a photon into the cavity mode (upward arrows) and loss of a photon from the cavity through the output mirror (downward arrows). Furthermore, the processes that start from a given state and end in a different one will decrease the probability of the state they are starting from and increase the probability of the state they are ending at. For example, the first term on the right-hand side describes emission of a photon into the cavity mode provided there are n photons already present before the emission event takes place. Since there will be $n + 1$ photons after the emission, this process decreases the probability of finding n photons, hence the minus sign. The total emission rate $\mathscr{A}(n+1)$ has a contribution from stimulated emission, the $\mathscr{A}(n)$ term, and another one from spontaneous emission, the $\mathscr{A}$ term. The third term on the right-hand side corresponds similarly to emission, conditioned on the presence of $n - 1$ photons in the cavity initially. After the emission, there will be n photons, hence the plus sign. The second term describes the loss of a photon through the cavity mirror, provided there are n photons initially. After the escape of a photon, there will be $n - 1$ photons; therefore, this term decreases $p(n)$. Finally, the last term corresponds similarly to a loss process, with initially $n + 1$ photons in the cavity. After the escape of a photon there will be n photons left, so this term increases the probability $p(n)$ of finding n photons in the cavity.

After this brief discussion of the meaning of the individual terms, we now turn our attention to the solution of the equation. Although it is possible to obtain a rather general time-dependent solution to Eq. (58), our main interest here is in the steady-state properties of the field. To obtain the steady-state photon statistics, we replace the time derivative with zero. Note that the right-hand side of the equation is of the form $F(n + 1) - F(n)$, where

$$F(n)=\kappa n p(n)-\frac{n\mathscr{A}}{1+n\mathscr{B}/\mathscr{A}}\,p(n-1) \tag{59}$$

simply meaning that in steady-state $F(n + 1) = F(n)$. In other words, $F(n)$ is independent of n and is, therefore, a constant c. Furthermore, the equation $F(n) = c$ has normalizable solution only for $c = 0$. From Eq. (59) we then immediately obtain

$$p(n)=\frac{\mathscr{A}/\kappa}{1+n\mathscr{B}/\mathscr{A}}\,p(n-1) \tag{60}$$

which is a very simple two-term recurrence relation to determine the photon-number distribution. Before we present the solution, a remark is called for here. The fact that $F(n) = 0$ and $F(n + 1) = 0$ hold separately is called the *condition of detailed balance*. As a consequence, we do not need to deal with all four processes affecting $p(n)$. It is sufficient to balance the processes connecting a pair of adjacent levels in Fig. 5, and instead of solving the general three-term recurrence relation resulting from the steady-state version of Eq. (58), it is enough to solve the much simpler two-term recursion, Eq. (60).

It is instructive to investigate the photon statistics in some limiting cases before discussing the general solution. Below threshold the linear approximation holds. Since only very small n states are

populated appreciably, the denominator on the right-hand side of Eq. (60) can be replaced by unity in view of $n\mathcal{B}/\mathcal{A} \ll 1$. Then

$$p(n) = p(0)\left(\frac{\mathcal{A}}{\kappa}\right)^n \tag{61}$$

The normalization condition $\sum_{n=0}^{\infty} p(n) = 1$ determines the constant $p(0)$, yielding $p(0) = (1 - \mathcal{A}/\kappa)$. Finally,

$$p(n) = \left(1 - \frac{\mathcal{A}}{\kappa}\right)\left(\frac{\mathcal{A}}{\kappa}\right)^n \tag{62}$$

Clearly, the condition of existence for this type of solution is $\mathcal{A} < \kappa$. Therefore, $\mathcal{A} = \kappa$ is the threshold condition for the laser. At threshold, the photon statistics change qualitatively and very rapidly in a narrow region of the pumping parameter. It should also be noted that below threshold the distribution function Eq. (62) is essentially of thermal character. If we introduce an effective temperature T defined by

$$\exp\left(-\frac{\hbar\omega_0}{kT}\right) = \frac{\mathcal{A}}{\kappa} \tag{63}$$

we can cast Eq. (62) to the form

$$p(n) = \left[1 - \exp\left(-\frac{\hbar\omega_0}{kT}\right)\right]\exp\left(-\frac{n\hbar\omega_0}{kT}\right) \tag{64}$$

This is just the photon-number distribution of a single mode in thermal equilibrium with a thermal reservoir at temperature T. The inclusion of a finite temperature-loss reservoir to represent cavity losses will not alter this conclusion about the region below threshold.

There is no really good analytical approximation for the region around threshold, although the lowest-order expansion of the denominator in Eq. (60) yields some insight. The solution with this condition is given by

$$p(n) = p(0)\left(\frac{\mathcal{A}}{\kappa}\right)^n \prod_{k=0}^{n}\left(1 - \frac{k\mathcal{B}}{\mathcal{A}}\right) \tag{65}$$

This equation clearly breaks down for $n > \mathcal{A}/\mathcal{B} = n_{\max}$, where $p(n)$ becomes negative. The resulting distribution is quite broad, exhibiting a long plateau and a rapid cutoff at $n_{\max}$. The broad plateau means that many values of n are approximately equally likely; therefore, the intensity fluctuations are large around threshold. The most likely value of $n = n_{\text{opt}}$ can be obtained from the condition $p(n_{\text{opt}} - 1) = p(n_{\text{opt}})$ since $p(n)$ is increasing before $n = n_{\text{opt}}$ and decreasing afterwards. This condition yields $n_{\text{opt}} = (\mathcal{A} - \kappa)/\mathcal{B}$, which is smaller by the factor $\kappa/\mathcal{A}$ than the value obtained from the full nonlinear equation [cf. Eq. (70) following].

The third region of special interest is the one far above threshold. In this region, $\mathcal{A}/\kappa \gg 1$ and the n values contributing the most to the distribution function are the ones for which $n \gg \mathcal{A}/\mathcal{B}$. We can then neglect 1 in the denominator of Eq. (60), yielding

$$p(n) = \exp\left(-\bar{n}\frac{\bar{n}^n}{n!}\right) \tag{66}$$

with $\bar{n} = \mathcal{A}^2/(\kappa\mathcal{B})$. Thus, the photon statistics far above threshold are poissonian, the same as for a coherent state. This, however, does not mean that far above threshold the laser is in a coherent state. As we shall see later, the off-diagonal elements of the density matrix remain different from those of a coherent state for all regimes of operation.

After developing an intuitive understanding of the three characteristically different regimes of operation, we give the general solution of Eq. (60), valid in all three regimes:

$$p(n)=p(0)\prod_{k=1}^{n}\frac{(\mathcal{A}/\kappa)}{(1+k(\mathcal{B}/\mathcal{A})} \tag{67}$$

The normalization constant $p(0)$ may be expressed in terms of the confluent hypergeometric function

$$p(0)=\left[\sum_{n=0}^{\infty}\frac{\left(\frac{\mathcal{A}}{\mathcal{B}}\right)!\left(\frac{\mathcal{A}^2}{\mathcal{B}\kappa}\right)^n}{\left(n+\frac{\mathcal{A}}{\mathcal{B}}\right)!}\right]^{-1}$$

$$=\left[F\left(1;\frac{\mathcal{A}}{\mathcal{B}}+1;\frac{\mathcal{A}^2}{\mathcal{B}\kappa}\right)\right]^{-1} \tag{68}$$

In Fig. 6, the photon-number distribution is displayed for various regimes of operation.

It is interesting to note that $p(n)$ is a product of n factors of the form $(\mathcal{A}/\kappa)/(1 + k\ \mathcal{B}/\mathcal{A})$. This is an increasing function of k as long as the factors are larger than 1 and decreasing afterward. The maximum of the distribution function can be found from the condition

$$\frac{(\mathcal{A}/\kappa)}{(1+n_m\mathcal{B}/\mathcal{A})}=1 \tag{69}$$

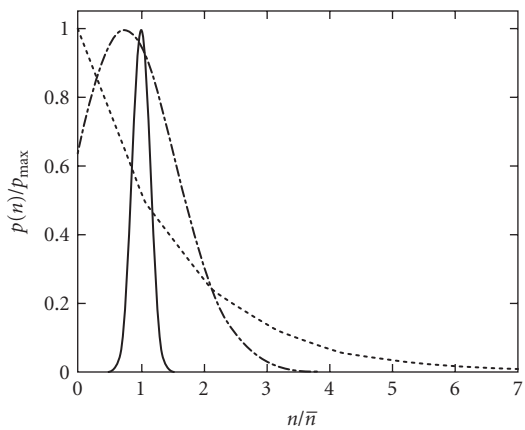

FIGURE 6 Photon statistics of the laser for various regimes of operation. Dotted line: laser 50 percent below threshold ($\mathcal{A}/\kappa = 1/2$), distribution thermal in character, Mandel $Q_M = 1$. Dot-dashed line: laser 10 percent above threshold, ($\mathcal{A}/\kappa = 1.1$), distribution is broad, $Q_M = 5$. Solid line: laser 100 percent above threshold ($\mathcal{A}/\kappa = 2$), distribution super-Poissonian, $Q_M = 1$. Since in the various regimes the actual photon numbers and $p(n)$ values differ by several orders of magnitude, in order to comparatively display the statistics in one figure, we plot $p(n)/p_{\max}$ versus $n\sqrt{n}$. This way the maximum of each curve is 1 and unity on the horizontal axis corresponds to the average photon number. $\mathcal{A}/\mathcal{B} = 50$ is used for all plots, for illustrative purposes only. For more realistic values, the above-threshold distributions are much narrower on this scale.

or

$$n_m = \frac{\mathcal{A}}{\mathcal{B}} \frac{\mathcal{A}-\kappa}{\kappa} \tag{70}$$

Clearly, for $\mathcal{A} < \kappa$ the maximum is at $n = 0$ and the distribution is monotonically decreasing, which is characteristic of a thermal distribution. This is in agreement with the previous findings for the below-threshold region. Around $\mathcal{A} \simeq \kappa$ the distribution quickly changes its character. The factor $\mathcal{A}/\mathcal{B}$ governs the magnitude of the photon number while $(\mathcal{A} - \kappa)/\kappa$ is a measure of how far away from threshold the laser is operating. Typical values for CW gas lasers (the He-Ne laser, for example) are $\mathcal{A}/\mathcal{B} \simeq 10^6$ and $\kappa \simeq 10^6$ Hz. Around threshold, $\mathcal{A} \simeq \kappa$ and the factors appearing in $p(n)$, given by Eq. (69), are effectively unity for a broad range of n. For example, for $\mathcal{A}/\kappa = 1.001$ (i.e., one-tenth of a percent above threshold), the factors are slightly above 1 for $1 < n < 1000$. So, in the threshold region, the distribution very quickly changes from a thermal one, dominated by the vacuum state, to a broad distribution with large intensity fluctuations. Farther above threshold the distribution becomes more and more peaked around n_m and becomes essentially poissonian for $\mathcal{A}/\kappa > 2$.

It is easy to obtain the mean photon number $\bar{n}$ from Eq. (67):

$$\bar{n} = \sum_{n=0}^{\infty} np(n) \frac{\mathcal{A}}{\mathcal{B}} = \frac{\mathcal{A}-\kappa}{\kappa} + \frac{\mathcal{A}}{\mathcal{B}} p(0) \tag{71}$$

Above threshold, $p(0) \ll 1$ and the last term becomes quickly negligible. Then $\bar{n}$ coincides with n_m, the maximum of the distribution. We can obtain $\overline{n^2}$ similarly. The result is

$$\overline{n^2} = \bar{n}^2 + \frac{\mathcal{A}^2}{\mathcal{B}\kappa} \tag{72}$$

Using Eq. (71), the variance can be expressed as

$$\sigma^2 = \overline{n^2} - \bar{n}^2 = \bar{n} \frac{\mathcal{A}}{\mathcal{A}-\kappa} \tag{73}$$

From here we see that the variance always exceeds that of a poissonian distribution ($\sigma^2 > \bar{n}$), but it approaches one far above threshold. A good characterization of the photon-number distribution is given by the Mandel Q_M parameter:

$$Q_M = \frac{\overline{n^2} - \bar{n}^2}{\bar{n}} - 1 \tag{74}$$

For our case, it is given by

$$Q_M = \frac{\kappa}{\mathcal{A}-\kappa} \tag{75}$$

Since $Q_M > 0$ above threshold, the field is superpoissonian. Very far above threshold, when $\mathcal{A} \gg \kappa$, Q_M approaches zero, which is characteristic of a poissonian distribution, again in agreement with our discussion of the far-above-threshold region.

Micromaser Photon Statistics As a first application of the micromaser master equation, Eq. (56), we shall study the steady-state photon statistics arising from it. To this end we take the diagonal $n = n'$ elements, and after regrouping the terms we obtain:

$$\begin{aligned} \dot{p}(n) = &-N_{\text{ex}} \sin^2(g\tau\sqrt{n+1})\, p(n) + (n_{\text{th}}+1)(n+1)\, p(n+1) - n_{\text{th}}(n+1)\, p(n) \\ &+ N_{\text{ex}} \sin^2(g\tau\sqrt{n})\, p(n-1) - (n_{\text{th}}+1) n p(n) + n_{\text{th}} n p(n-1) \end{aligned} \tag{76}$$

Here the overdot stands for derivative with respect to the scaled time $t' = \kappa t$. $N_{ex} = r/\kappa$ is the number of atoms traversing the cavity during the lifetime of the cavity field, and the diagonal matrix elements of the density operator $p(n) = \varrho_{nn}$ are the probabilities of finding n photons in the cavity. The various processes in the right-hand side of this equation are again visualized in Fig. 5. They have the structure $F(n+1) - F(n)$ where $F(n+1)$ corresponds to the processes connecting $p(n+1)$ to $p(n)$. In the steady state the left-hand side is zero and $F(n+1) = F(n)$, yielding $F(n) =$ constant. The only normalizable solution to the photon statistics arises when this constant is zero, $F(n) = 0$. Once again, this is the condition of detailed balance because the probability flows between adjacent levels are separately balanced. More explicitly, this leads to the following recurrence relation for the photon-number probabilities:

$$p(n) = \frac{N_{ex} \sin^2(g\tau\sqrt{n})/n + n_{th}}{n_{th} + 1} p(n-1) \tag{77}$$

The solution to this simple recurrence relation is straightforward:

$$p(n) = p(0) \prod_{i=1}^{n} \frac{N_{ex} \sin^2(g\tau\sqrt{i})/i + n_{th}}{n_{th} + 1} \tag{78}$$

where $p(0)$ is determined from the normalization condition $\sum_{n=0}^{\infty} p(n) = 1$. The photon-number distribution $p(n)$ versus n can be multipeaked in certain parameter regimes. This can be easily understood on the basis of Fig. 5. The gain processes (upward arrows) balance the loss (downward arrows). Since the gain is an oscillatory function of n, several individual peaks [with the property $p(n+i) = p(n)$] will develop for those values of n where the gain perfectly balances the loss. The resulting mean photon number (first moment of the distribution) and photon-number fluctuations (second moment Q_M) versus the scaled interaction parameter $\theta = g\tau\sqrt{N_{ex}}$ are displayed in Fig. 7.

The mean photon number is an oscillatory function of the scaled interaction time. The oscillations correspond to subsequent Rabi cycles the atoms are undergoing in the cavity as function of the interaction time. The first threshold occurs at $\theta = 1$; the higher ones occur where θ is approximately an integer multiple of 2π. Around the thresholds the micromaser field is superpoissonian; in the parameter region between the thresholds it is subpoissonian, which is a signature of its nonclassicality.

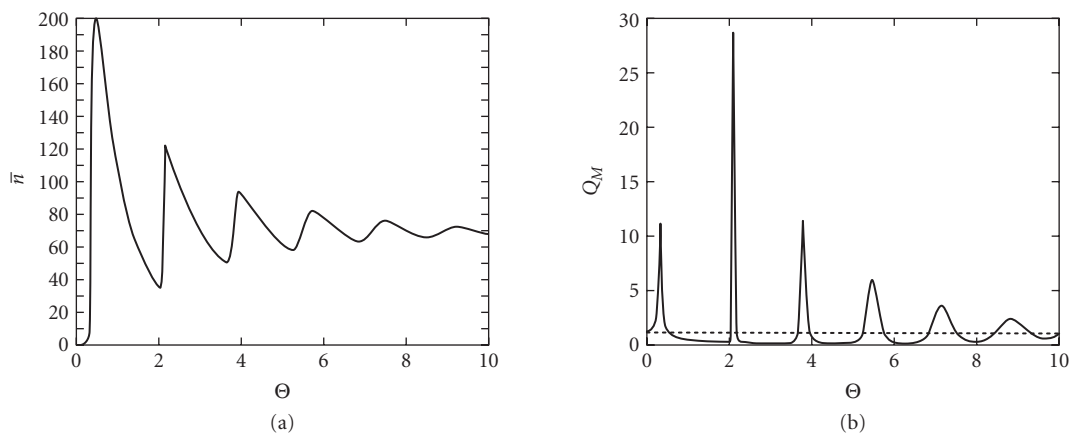

FIGURE 7 (*a*) Mean photon number and (*b*) Mandel Q_M parameter versus interaction parameter for the micromaser, for $N_{ex} = 200$.

Physics off the Main Diagonal: Spectrum and Linewidth

In the subsection on laser photon statistics we have shown that the laser has poissonian photon statistics far above threshold, just as a coherent state would. However, it is erroneous to conclude from this that the laser field is in a coherent state far above threshold. Only the intensity of the laser becomes stabilized due to a delicate balance of the nonlinear gain and loss. Any deviation from the steady-state intensity induces a change that tries to restore the steady-state value; as a result, the intensity is locked to this value. The phase of the field, on the other hand, evolves freely and is not locked to any particular value. In fact, it performs a random walk due to the separate spontaneous emission events. Each such event contributes a small random phase change to the instantaneous phase of the field. The mean of these changes averages to zero, but the mean of the square of these changes remains finite. As a result, the phase undergoes a diffusionlike process and will become uniformly distributed over the 2π interval. Any information contained in the instantaneous phase will be erased in this process. The time scale for the decay of the phase information is given by the rate of the phase diffusion. In the following, we shall determine this characteristic time scale, the so-called phase diffusion constant for the laser and micromaser.

Spectral Properties of the Laser Field The decay of the phase information can be directly read out from the temporal behavior of the two-time correlation function of the field amplitude:

$$g^{(1)}(t_0+t,t_0)=\frac{\langle a^\dagger(t_0+t)a(t_0)\rangle}{\langle a^\dagger(t_0)a(t_0)\rangle} \tag{79}$$

With increasing time difference between their amplitudes, the fields become less and less correlated since spontaneous emission randomizes their phases. At steady state, the two-time correlation function [Eq. (79)] depends only on the time difference t and is independent of the choice of the initial time t_0.

A quantum regression "theorem,"[88] based on a system-reservoir factorization of the density matrix, was developed to permit the time evolution of the two-time correlation function at steady state to be calculated from the time evolution of the single-time correlation function for a Markov process. The unusual success of this procedure (see Ref. 89 for a comparison between experiment and theory for the phase linewidth, the intensity linewidth, the photo-count distribution, and the spectral moments) requires additional explanation. This was supplied in a proof that regression is valid when the system is markovian.[90] In the quantum case, the system is only approximately markovian. But this assumption has already been made in all cases for which solutions have been found. Therefore, it is sufficient for us to study the time evolution of the amplitude itself:

$$\langle a^\dagger(t)\rangle=\sum_{n=0}^{\infty}\sqrt{n+1}\,\varrho_{nn+1} \tag{80}$$

At this point it is useful to define a column vector with the components $\varrho_n^{(k)}\equiv\varrho_{nn+k}$ This way, we simply arrange the elements of the kth diagonal in the form of a vector. For example, elements on the first side diagonal correspond to $k=1$, and so on. Let us note that the equation of motion for the off-diagonal matrix elements of the density operator can now be written in a simple matrix form

$$\dot{\varrho}_n^{(k)}=A_{nn'}\,\varrho_{n'}^{(k)} \tag{81}$$

where summation is implied over repeated indexes and the matrix elements $A_{nn'}$ can be read out from Eq. (49). They are given by

$$A_{nn'}=-\left[\frac{\mathcal{N}'_{nn+k}\mathcal{A}}{1+\mathcal{N}_{nn+k}\mathcal{B}/\mathcal{A}}+\kappa\left(n+\frac{k}{2}\right)\right]\delta_{nn'}+\frac{\sqrt{n(n+k)}\mathcal{A}}{1+\mathcal{N}_{n-1n+k-1}\mathcal{B}/\mathcal{A}}\delta_{nn'+1}$$
$$+\kappa\sqrt{(n+1)(n+k+1)}\,\delta_{nn'-1} \tag{82}$$

Clearly, $A_{nn'}$ is a tridiagonal matrix. Due to its linearity, we can look for the solution of Eq. (81) by the simple exponential Ansatz, $\varrho_n^{(k)}(t) = e^{-\lambda t}\varrho_n^{(k)}(0)$. With this substitution, Eq. (81) can be written in the form of an eigenvalue equation to determine λ,

$$\lambda \varrho_n^{(k)} = -\sum_{n-1}^{n+1} A_{nn'} \varrho_{n'}^{(k)} \tag{83}$$

We restrict the following treatment to $k = 1$ because that is what we need for the calculation of the $g^{(1)}$ correlation function. Higher-order correlation functions, $g^{(k)}$ with $k > 1$, are related to $\varrho_n^{(k)}$ with $k > 1$. From the structure of the $-A$ matrix, one can show that all eigenvalues are positive. There is a smallest eigenvalue, which we denote by D. This eigenvalue will dominate the longtime behavior of the field amplitude, as can easily be seen from the following considerations. Let us denote the set of eigenvalues by $\{D, \lambda_j\}$ with $j = 1, 2, 3, \ldots$. Then $\varrho_n^{(1)}(t)$ can be written as

$$\varrho_n^{(1)}(t) = \varrho_{n0}^{(1)}(0)\exp(Dt) + \sum_{j=1}^{\infty} \varrho_{nj}^{(1)}(0)\exp(-\lambda_j t) \tag{84}$$

From this we see that, indeed, the longtime behavior of the off-diagonal elements will be governed by the first term, since the other terms decay faster according to our assumption of D being the smallest positive eigenvalue. Therefore, our task is reduced to the determination of D. In order to obtain an analytical insight, we can proceed as follows. First, let us note that in the longtime limit all elements of the vector $\varrho_n^{(1)}(t)$ decay the same way—they are proportional to $\exp(-Dt)$. Therefore, the sum of the elements also decays with the same rate, D, in this limit. It is quite easy to obtain an equation of motion for the sum of the elements. Starting from Eq. (81) and using Eq. (82) for the case $k = 1$, we immediately obtain

$$\dot{\varrho}^{(1)} = -\sum_{n=0}^{\infty}\left[\frac{n+3/2-\sqrt{(n+1)(n+2)}}{1+(n+3/2)\mathcal{B}/\mathcal{A}}\mathcal{A} + \kappa(n+1/2-\sqrt{n(n+1)})\right]\varrho_n^{(1)} \tag{85}$$

Here we introduced the notation $\sum_{n=0}^{\infty}\varrho_n^{(1)} = \varrho^{(1)}$ and used the fact that $\mathcal{N}'_{nn+1} = n+3/2+\mathcal{B}/(8\mathcal{A}) \approx n+3/2$ and $\mathcal{N}_{nn+1} = n+3/2+\mathcal{B}/(16\mathcal{A}) \approx n+3/2$ since $\mathcal{B}/\mathcal{A} \approx 10^{-6}$and can therefore safely be neglected next to 3/2. In the longtime limit the time derivative on the left-hand side can simply be replaced by $-D$ due to Eq. (84). It is also plausible to assume that in the same limit those values of n will contribute the most that lie in the vicinity of $\bar{n}$. Then we can expand the coefficients around the steady-state value of the photon number. This is certainly a good approximation in some region above threshold. The key point is that after the expansion the coefficients of $\varrho_n^{(1)}$ on the right-hand side become independent of the summation index n and can be factored out from the sum. Then, after the summation, the quantity $\varrho^{(1)}$ also appears on the right-hand side of the equation:

$$D\varrho^{(1)} = \frac{\mathcal{A}+\kappa}{8\bar{n}}\varrho^{(1)} \tag{86}$$

From this we can simply read out the decay rate:

$$D = \frac{\mathcal{A}+\kappa}{8\bar{n}} \tag{87}$$

This quantity, called the *phase diffusion coefficient*, plays a crucial role in determining the transient behavior of the laser as well as its spectral properties. It exhibits the characteristic line narrowing for high intensity, first found by Schawlow and Townes.[80] The mean amplitude, Eq. (80), can now be written as

$$\langle a^{\dagger}(t)\rangle = e^{-Dt}\langle a^{\dagger}(0)\rangle \tag{88}$$

The decay of any initial coherent component of the laser field is governed by the phase diffusion constant, due to the randomization of the initial phase information. The randomization is due to two separate processes, as can be read out from the analytical expression, Eq. (87) of the phase diffusion constant. The part proportional to the spontaneous emission rate $\mathcal{A}$ is due to the random addition of photons to the field via spontaneous emission; the part proportional to the cavity decay rate is due to leaking of vacuum fluctuations into the cavity through the output mirrors. Both processes randomize the phase of the initial field; as a result, the phase performs a random walk with a diffusion rate given by Eq. (87). Ultimately, of course, vacuum fluctuations are also responsible for spontaneous emission.

The phase diffusion constant also determines the linewidth of the spectrum of the laser field. Using the quantum regression theorem, we immediately find that the (nonnormalized) steady-state field correlation function is given by

$$g^{(1)}(t_0+t,t_0)=\left\langle a^\dagger(t_0+t)a(t_0)\right\rangle=\bar{n}\exp(i\omega_0 t-Dt) \tag{89}$$

where ω_0 denotes the operating frequency of the laser, as before. The power spectrum is given by the Fourier transform of the field correlation function:

$$S(\omega)=\frac{1}{\pi}\mathrm{Re}\int_0^\infty g^{(1)}(t_0+t,t_0)e^{-i\omega t}dt=\frac{\bar{n}}{\pi}\frac{D}{(\omega-\omega_0)^2+D^2} \tag{90}$$

This is a lorentzian spectrum centered around the operating frequency, $\omega=\omega_0$. The full width at half-maximum (FWHM) is given by $2D$. Figure 8 depicts the normalized spectrum $S(\omega)/S(\omega_0)$ versus the detuning $\Delta=(\omega-\omega_0)/D$.

It should be emphasized that our method of obtaining the preceding analytical approximations is justified only if the mean photon number is large, the photon-number distribution consists of a single large peak, and cross-coupling between intensity and phase, arising from the nonlinearity of the gain very far above threshold, is negligible. These conditions are met for a laser in some region above threshold. Near the threshold, however, the intensity fluctuations cannot be neglected. From

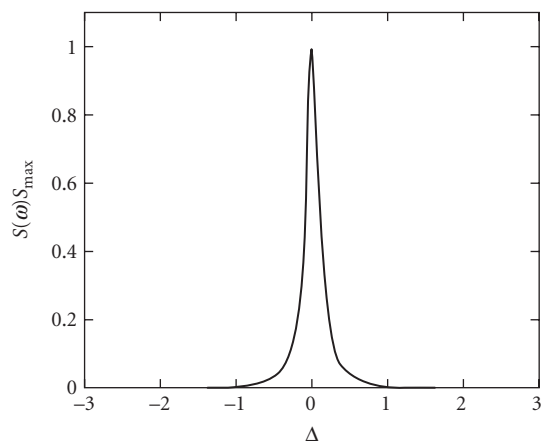

FIGURE 8 Laser spectrum $S(\omega)/S_{\max}$ versus detuning $\Delta=(\omega-\omega_0)/\kappa$, for a laser 100 percent above threshold (note that detuning is in units of bare-cavity linewidth). For our parameters the spectral width D is about 1 percent of the bare-cavity linewidth, an example of the Schawlow-Townes narrowing

numerical studies[91] it was concluded that their contribution to the linewidth is approximately equal to the phase diffusion constant, and the linewidth in this region is about twice what is predicted by Eq. (90); i.e., it is $4D$; and far above threshold (for $\mathcal{A}\kappa > 2$), the linewidth is smaller than the prediction of Eq. (90). These numerical findings are confirmed by a recent analytical approach to the problem.[92] One of the earliest quantum calculations of the laser linewidth[69] was based on the quantum theory of noise sources.[70] The laser linewidth above threshold was established to be due mostly to phase noise,[69] and it was explained that the factor of 2, too large, was obtained by many previous authors because they had permitted amplitude fluctuations, which were valid near threshold but not far above. These ideas were confirmed by analytic calculations below and above threshold[93] and by a numerical solution of the associated Fokker-Planck equation.[94,95] Moreover, the effects of laser detuning on the linewidth were determined without assuming that the light field decays much slower than the atomic decay rates. It was found that the effective linewidth was a harmonic mean between the field and electronic decay rates, as shown in Eq. (35) of Ref. 69.

The calculations of the phase linewidth done in this section are equivalent to the quasilinear approximation employed in the Langevin noise source procedure in Ref. 93 and shown in Ref. 94 to be valid for dimensionless pump rates $p > 10$. Below threshold, $p < -10$, the components of the electromagnetic field can be treated as uncoupled gaussian variables, leading to the Schawlow-Townes formula. Only the region in the immediate vicinity of threshold requires careful analysis. In that region, it is shown in footnote 10 in Ref. 93 that the coefficients in the Fokker-Planck equation can be expanded in powers of n, retaining only the first nonlinear term. The result then reduces to the rotating-wave Van der Pol oscillator. One advantage of this reduction is that the equation can be scaled in time and in amplitude, leaving the dimensionless pump parameter p as the only remaining parameter. This greatly reduces any subsequent numerical calculations. The ability to retain only one nonlinear term is based only on the requirement that we are dealing with a good oscillator—that is, one whose signal-to-noise ratio is large. Equivalent approximations can be introduced in the density matrix treatment, as well.

The assumption made here that the phase linewidth comes predominantly from the smallest decay eigenvalue was established in Ref. 94, where the actual line shape is shown to be a sum of lorentzians, and the percentage from each lorentzian is calculated. The intensity fluctuations are also expressed as a sum of lorentzians but several modes contribute, not just the lowest. The percentage in each is given in Ref. 94. Part of the reason for this is that the modes approach degeneracy in pairs as one moves above threshold. The lifting of such a degeneracy was shown in Ref. 96 to be associated with a phase transition. Since our system is finite, the phase change occurs gradually and can be observed. The view of lasing as a phase transition will be explored in more detail in Sec. 23.5.

Spectral Properties of the Micromaser Field If we take the n, $n+1$ matrix elements of Eq. (57), then, following the methods of the previous subsection, it is straightforward to derive the diffusion constant. In particular, elements of the first side diagonal can again be arranged in the form of a column vector, and this vector again satisfies an equation of motion similar to Eq. (81), with an appropriate redefinition of the tridiagonal matrix appearing in the equation:

$$\begin{aligned} A_{nn'} = &-\{r[1-\cos(g\tau\sqrt{n+1})\cos(g\tau\sqrt{n+2})]+\kappa(2n_{\text{th}}(n+1)+n+1/2)\}\delta_{nn'} \\ &+(r\sin(g\tau\sqrt{n})\sin(g\tau\sqrt{N+1})+\kappa n_{\text{th}}\sqrt{n(n+1)})\delta_{nn'+1} \\ &+\kappa(n_{\text{th}}+1)\sqrt{(n+1)(n+2)}\delta_{nn'-1} \end{aligned} \tag{91}$$

The exponential Ansatz for the decay of the column vector again turns the equation of motion into an eigenvalue equation for the matrix A and the longtime behavior will again be governed by the smallest eigenvalue, which we denote by D. Summing over all elements of the resulting eigenvalue

equation and replacing the coefficients on the right-hand side by their longtime value—that is, expanding the coefficients around $n=\bar{n}$—will finally yield

$$D=2r\sin^2\left(\frac{g\tau}{4\sqrt{\bar{n}}}\right)+\kappa\frac{(2n_{\text{th}}+1)}{8\bar{n}} \tag{92}$$

for the phase diffusion constant of the micromaser. Here $\bar{n}$ is the mean photon number of the (single-peaked) distribution. This expression was first derived by Scully et al.[97] It leads to a lorentzian spectrum similar to Eq. (90) but with D appropriately replaced by that of the micromaser. It should be noted, however, that the analytical formula has a more restricted validity than in the case of the laser. Namely, in the case of the micromaser, the photon-number distribution can be multipeaked, and the simple expansion around the $\bar{n}$ value corresponding to a single dominating peak may not hold. For this more general case several numerical approaches have been developed (see Ref. 98). When Eq. (92) is valid it coincides with the results of the numerical calculations.

For small values of the argument in the sine function, Eq. (92) can be cast to a form which is formally identical to the usual laser phase diffusion constant [99][cf. Eq. (87)]:

$$\begin{aligned} D&=r\frac{g^2\tau^2}{8\bar{n}}+\kappa\frac{2n_{\text{th}}+1}{8\bar{n}}\\ &=\frac{\mathcal{A}+\kappa(2n_{\text{th}}+1)}{8\bar{n}} \end{aligned} \tag{93}$$

Here we introduced the small signal gain $\mathcal{A}\equiv rg^2\tau^2$, in analogy to the laser gain. However, for other values of the argument the first term in Eq. (92) may dominate, and the phase diffusion constant can exceed the bare-cavity linewidth, which is a unique quantum feature of the micromaser and makes it distinctly different from the classical Schawlow-Townes-type behavior.

Without going into the specifics, we just mention a few other aspects of the quantum theory of the micromaser. As we have just seen a steady state is reached due to the equilibrium between the gain and loss processes. In some cases, however, a steady state can be reached even in a lossless cavity. This happens if the probability flow in Fig. 5 due to the gain process is interrupted for some value of the interaction parameter. The upward flow is interrupted when

$$g\tau\sqrt{n_q+1}=q\pi \tag{94}$$

and the downward flow is interrupted when

$$g\tau\sqrt{n_q}=q\pi \tag{95}$$

with $q=1,2,\ldots$ in both cases. They are called the *upward* and *downward trapping state*, respectively.[100] In such cases the state of the field is a number state. The signature of the number state is a large maximum in the linewidth at the corresponding interaction parameter. It can easily be understood qualitatively: since the state of the field is a number state, it cannot have any phase information. Therefore, the phase randomizes on a very rapid time scale; in other words, the phase correlations decay very rapidly, and a large phase diffusion constant ensues. Further, if the atoms are injected in a coherent superposition of their upper and lower levels in the cavity then, under certain conditions, the so-called tangent and cotangent states of the field may develop.[101] Finally, it should be mentioned that the master equations Eqs. (49) and (56) hold only for the case when the time interval between consecutive atomic injections is completely random. Other arrival times statistics, including the case of regular injections, have been investigated by a number of authors.[102] A closely related area of recent theoretical studies pertains to the detection of the statistical properties of the (experimentally inaccessible) intracavity field via monitoring the statistics of the outgoing atoms for poissonian[103] as well as nonpoissonian[104] pumping. For regular (subpoissonian) pumping, transient oscillations in field correlation function and a corresponding multipeaked spectrum were predicted.[105]

Most of the predictions of this theory have been confirmed by experiments. For example, trapping states have been observed in recent experiments by the Garching group.[106] Without providing an exhaustive list, we just refer the reader to recent progress in the experimental department.[107]

Other Approaches

So far we have considered laser theory based on a density-operator approach. An equivalent approach to a laser theory can be formulated using a Heisenberg-Langevin approach. In this approach explicit equations of motion are derived for the field operator.

The quantum-noise operator formalism was presented in essentially its final form by Lax at the 1965 meeting on the *Physics of Quantum Electronics*.[69] There, it was applied to the laser, calculating, the laser linewidth in its most general form. For the general theory, see the 1966 Brandeis lecture notes of Lax.[71]

In the present formulation, our goals are more specific—namely, the Heisenberg-picture quantum theory of the laser. To that end, we will here give a quantum-noise treatment along the lines of that followed in the previous subsection—namely, a single laser mode damped at a rate κ by a (dissipative) reservoir and driven by atoms injected into the laser cavity at random times t_j.

First we discuss the simple example of damping of the field by a reservoir and derive the quantum Langevin equation for the field operator. We then discuss the gain noise in a laser and derive the laser linewidth.

Damping of Field by Reservoir We consider the damping of a single-mode field of frequency ν interacting with a reservoir consisting of simple harmonic oscillators. The system describes, for example, the damping of a single-mode field inside a cavity with lossy mirrors. The reservoir in this case consists of a large number of phononlike modes in the mirror.

The field is described by the creation and destruction operators $a^\dagger$ and a, whereas the harmonic oscillators of frequency $\nu_k = ck$ are described by the operators $b_k^\dagger$ and b_k. The field-reservoir system evolves in time under the influence of the total hamiltonian:

$$\mathcal{H} = \hbar\omega_0(a^\dagger a + \frac{1}{2}) + \hbar\sum_k \nu_k\left(b_k^\dagger b_k + \frac{1}{2}\right) + \hbar\sum_k g_k(ab_k^\dagger + b_k a^\dagger) \tag{96}$$

Here g_k *are* the coupling constants and we have made the rotating-wave approximation. We are interested in the evolution of the field operator a. The Heisenberg equations of motion for the field and reservoir are

$$\dot{a}(t) = -i\omega_0 a(t) - i\sum_k g_k b_k(t) \tag{97}$$

$$\dot{b}_k(t) = -i\nu_k b_k(t) - ig_k a(t) \tag{98}$$

The equation for b_k can be formally solved, and the resulting expression is substituted in Eq. (97). In the Weisskopf-Wigner approximation, the annihilation operator in the interaction picture $a = a(t)\exp[i\omega_0(t-t_0)]$ satisfies a Langevin equation

$$\dot{a} = -\frac{\kappa}{2}a + F(t) \tag{99}$$

where

$$F(t) = -i\sum_k g_k b_k(0)\exp[-i(\nu_k - \omega_0)(t-t_0)] \tag{100}$$

is a noise operator. Equation (99) clearly indicates that the damping of the field (represented by the term $-\kappa a/2$) is accompanied by noise.

For the damping of the single-mode field inside a cavity via transmission losses, the damping constant κ is related to the quality factor Q of the cavity via $\kappa = \omega_0/Q$.

Atomic (Gain) Noise and Laser Linewidth As discussed earlier, the natural linewidth of the laser arises due to spontaneous emission by the atoms. In the density-operator approach, a fully nonlinear treatment was followed. Here, we present a simple linear analysis to calculate the laser linewidth in the Heisenberg-Langevin approach. We assume that the atoms are long lived, and that they interact with the cavity field for a time τ. This treatment allows us to include the memory effects inside a laser, and is one of the simplest examples of a nonmarkovian process.[108,109]

We start with the hamiltonian describing the atom-field interaction:

$$\mathcal{H} = \mathcal{H}_F + \mathcal{H}_{\text{atom}} + \hbar g \sum_i \{\sigma^i a^\dagger N(t_i, t, \tau) + Hc\} \tag{101}$$

where $\mathcal{H}_F$ and $\mathcal{H}_{\text{atom}}$ describe the field and atoms, respectively; g is the atom-field coupling constant; and σ_i is the lowering operator for the ith atom; Hc is the injunction to add the Hermitian conjugate. The operators a and $a^\dagger$ represent the annihilation and creation operators, and $N(t_i, t, \tau)$ is a notch function which has the value

$$N(t_i, t, \tau) = \begin{cases} 1 & \text{for } t_i \le t < \tau \\ 0 & \text{otherwise} \end{cases} \tag{102}$$

Using this hamiltonian, we write the equations for the atom-field operators in the interaction picture as

$$\begin{aligned} \dot{a} &= -ig \sum_i \sigma^i N(t_i, t, \tau) - \frac{1}{2}\kappa a(t) + F_\kappa(t) \\ \dot{\sigma}^i &= igN(t_i, t, \tau)\sigma_z^i a(t) \end{aligned} \tag{103}$$

where the effects of cavity damping are determined by the cavity decay rate κ and the associated Langevin noise source F_κ. Integrating the equation for the atom operator and substituting it into that for the field operator, we obtain

$$\dot{a}(t) = \int_{-\infty}^{t} dt' \alpha(t, t') a(t') - \frac{1}{2}\gamma a + F_\alpha(t) + F_\kappa(t) \tag{104}$$

where

$$\alpha(t, t') = g^2 \sum_i N(t_i, t, \tau) N(t_i, t', \tau) \sigma_z^i(t') \tag{105}$$

$$F\alpha(t) = -ig \sum_i N(t_i, t, \tau) \sigma^i(t_i) \tag{106}$$

Here, the noise operator Eq. (106) may be seen to have the moments

$$\langle F_\alpha(t) \rangle = 0 \tag{107}$$

$$\langle F_\alpha^\dagger(t) F_\alpha(t') \rangle = g^2 \sum_{ij} N(t_i, t, \tau) N(t_i, t', \tau) \langle \sigma^{\dagger i}(t_i) \sigma^j(t_j) \rangle \tag{108}$$

Because we are injecting our lasing atoms in the upper state, the atomic average is given by $\langle \sigma^{\dagger i}(t_i) \sigma^j(t_j) \rangle = \delta_{ij}$. After replacing the sum upon i in Eq. (108) by an integration over injection times t_j, we find

$$\langle F_\alpha^\dagger(t) F_\alpha(t') \rangle = rg^2 \{N(t' - \tau, t, \tau)[t - (t' - \tau)] - N(t', t, \tau)[t - (t' + \tau)]\} \tag{109}$$

where r is the atomic injection rate. The phase variance can then be calculated through the noise operator product:

$$\langle \phi^2(t) \rangle = -\frac{1}{2\pi} \int_0^t dt' \int_0^t dt'' \langle F^\dagger(t') F(t'') \exp\{i[\phi(t') - \phi(t'')]\} \rangle \tag{110}$$

On insertion of Eq. (109) into Eq. (110), the expression for the generalized maser phase diffusion noise $\langle \phi^2(t) \rangle$ is found to be

$$\langle \phi^2(t) \rangle = \left(\frac{\mathcal{A}}{2\bar{n}} \right) \left[\left(\frac{t^2}{\tau} - \frac{t^3}{3\tau^2} \right) \theta(\tau - t) + \left(t - \frac{\tau}{3} \right) \theta(t - \tau) \right] \tag{111}$$

Here $\mathcal{A} = rg^2\tau^2$ is the small-signal gain of the maser [cf. Eq. (93), with $n_{th} = 0$ and using that in steady state $\mathcal{A} = \kappa$]. In the case involving atoms which are injected at random times t_i but which decay via spontaneous emission to far-removed ground states at a rate γ, a similar but more complicated analysis can be carried out. The result in this case is given by

$$\langle \phi^2(t) \rangle = \left(\frac{\mathcal{A}}{2\bar{n}} \right) [t + \gamma^{-1}(e^{-\gamma} - 1)] \tag{112}$$

Here $\mathcal{A} = 2rg^2/\gamma^2$ is the small-signal gain of the laser [cf. Eq. (50)]. In both of the preceding cases, we find that for times $t = t_m$ small compared to the atomic lifetime, the phase diffusion is quadratic in the measurement time t_m; that is, we now have a phase error which goes as

$$\Delta\phi^2 = \left(\frac{\mathcal{A} t_m}{2n} \right) \left(\frac{\gamma t_m}{2} \right) \tag{113}$$

Therefore, we see that the quantum noise due to spontaneous emission is reduced from the Schawlow-Townes linewidth $2D = \mathcal{A}/2\bar{n}$ by the factor $\gamma t_m/2$, which can be a significant reduction for short measurement times. For times long compared to the atomic lifetime, however, the Schawlow-Townes result is obtained from both Eqs. (111) and (112) as expected.

23.5 THE LASER PHASE-TRANSITION ANALOGY

Considerations involving the analogies between phase transitions in ferromagnets, superfluids, and superconductors have emphasized the similarities between these systems near their critical temperatures.[110]

A natural comparison can be made between second-order phase transitions, such as the order-disorder transitions of ferromagnetic and ferroelectric materials or the vapor-liquid transition of a pure fluid, and the laser threshold. As we have discussed in Sec. 23.4, the state of a laser changes abruptly upon passing through the threshold point. This point is characterized by a threshold population inversion.

The physical basis for this similarity becomes evident when it is recalled that the usual treatments of laser behavior are self-consistent theories. In the laser analysis we assume that each atom evolves in a radiation field due to all the other atoms, and then calculate the field produced by many such evolving atoms in a self-consistent fashion. In this way the laser problem is similar to that of a ferromagnet, in which each spin sees a mean magnetic field due to all the other spins and aligns itself accordingly, thus contributing to the average magnetic field.

Following this point of view, we can discuss the laser theory using the language of second-order phase transitions.

The density matrix of the laser field obeys Eq. (49). The time dependence of the expectation value $\bar{E}$ of the electric field operator $E=(a+a^\dagger)$ is there given by the following equation:

$$\dot{\bar{E}}=\frac{1}{2}(\mathscr{A}-\kappa)\bar{E}-\frac{\mathscr{B}}{2}\overline{E^3} \tag{114}$$

Here we have assumed that the laser is operating close to threshold ($\mathscr{B}\bar{n}/\mathscr{A}\ll 1$) so that we retain only the terms proportional to $\mathscr{B}$. In addition, we assume $\bar{E}\gg 1$. We can then replace $\bar{E}^3$ by $\bar{E}^3$ and Eq. (114) becomes the well-known result of Lamb's semiclassical theory. The steady-state properties of the laser oscillator are described by the following equation of state:

$$(\mathscr{A}-\kappa)\bar{E}-\mathscr{B}\overline{E^3}=0 \tag{115}$$

The threshold condition is given by $\mathscr{A}=\kappa$ as before. Upon putting $\mathscr{A}=a\sigma, \mathscr{B}=b\sigma$, and $\kappa=a\sigma_t$ where σ_t is the threshold population inversion, the steady-state solution of Eq. (115) is

$$\begin{aligned} &\bar{E}=0 && \text{if } \sigma-\sigma_t<0 \text{ (below threshold)} \\ &\bar{E}=\left[\frac{a}{b}\left(\frac{\sigma-\sigma_t}{\sigma}\right)^{1/2}\right] && \text{if } \sigma-\sigma_t>0 \text{ (above threshold)} \end{aligned} \tag{116}$$

Equation (116) is formally identical to the equation for a ferromagnet in the Weiss mean-field theory. The electric field E corresponds to the static magnetization M, which is the order parameter in the ferromagnetic transition. The quadratic polarization $P=(\mathscr{A}\bar{E}-\mathscr{B}\overline{E^3})/2$ in Eq. (115) corresponds to the magnetic field H generated by a magnetization M, and the term $\kappa\bar{E}/2$ corresponds to a local magnetic field which is assumed proportional to M in the mean-field theory. Furthermore, the steady-state points depend $\sigma-\sigma_t$ in the same way that M in the ferromagnetic case depends on $T-T_c$, where T_c is the critical temperature. Therefore, σ and σ_T correspond to T and T_c, respectively. The similarity between these two systems is summarized in Table 1 and illustrated in Fig. 9.

We recall that the probability density $P(M)$ for a ferromagnetic system with magnetization M near a phase transition is given by, in thermal equilibrium,

$$P(M)=N''\exp\left(-\frac{F(M)}{k_B T}\right) \tag{117}$$

where

$$F(M)=\frac{1}{2}c(T-T_c)M^2+\frac{1}{4}dTM^4 \tag{118}$$

is the free energy. In the corresponding laser analysis, the probability density for the electromagnetic field $P(E)$ is derived in the form

$$P(E)=N'\exp\left(-\frac{G(E)}{k_B\sigma}\right) \tag{119}$$

For this purpose we transform the laser equation for the density matrix for the field [Eq. (49)] into an equivalent equation in terms of the $P(\alpha,\alpha^*)$ representation defined by

$$\rho=\int d^2\alpha P(\alpha,\alpha^*)|\alpha\rangle\langle\alpha| \tag{120}$$

where $|\alpha\rangle$ is an eigenstate of the annihilation operator a with eigenvalue α. The P representation allows us to evaluate any normally ordered correlation function of the field operators using the

TABLE 1 Summary of Comparison between the Laser and a Ferromagnetic System Treated in a Mean-Field Approximation

Parameter	Ferromagnet	Laser
Order parameter	Magnetization M	Electric field strength E
Reservoir variable	Temperature T	Population inversion σ
		Threshold inversion σ_t
Coexistence curve*	$M=\Theta(T_c-T)\left[\frac{c}{d}\frac{T-T_c}{T}\right]^{1/2}$	$E=\Theta(\sigma-\sigma_t)\left[\frac{a}{b}\frac{\sigma-\sigma_t}{\sigma}\right]^{1/2}$
Symmetry breaking mechanism	External field H	Injected signal S
Critical isotherm†	$M=\left[\frac{H}{dT_c}\right]^{1/2}$	$E=\left[\frac{2S}{b\sigma_t}\right]^{1/2}$
Zero field susceptibility*	$X\equiv\left(\frac{\partial M}{\partial H}\right)\Big\|_{H=0}$	$\xi\equiv\left(\frac{\partial E}{\partial S}\right)\Big\|_{S=0}$
	$=\Theta(T_c-T)[2c(T_c-T)]^{-1}$	$=\Theta(\sigma_t-\sigma)\left[\frac{a(\sigma_t-\sigma)}{2}\right]^{-1}$
	$+\Theta(T-T_c)[c(T-T_c)]^{-1}$	$+\Theta(\sigma-\sigma_t)[a(\sigma-\sigma_t)]^{-1}$
Thermo-dynamic potential	$F(M)=\frac{1}{2}c(T-T_c)M^2$	$G(E)=-\frac{a}{4}(\sigma-\sigma_t)E^2$
	$+\frac{1}{4}dTM^4$	$+\frac{1}{8}b\sigma E^4$
	$-HM+F_0$	$-SE+G_0$
Statistical distribution	$P(M)=N''\exp\left(-\frac{F(M)}{k_BT}\right)$	$P(E)=N'\exp\left(-\frac{G(E)}{k_B\sigma}\right)$

*Θ ( ) is Heaviside's unit step function.
†Value of order parameter at critical point.

methods of classical statistical mechanics. The quantity $P(\alpha,\alpha^*)$ represents the probability density for finding the electric field corresponding to α.

Near threshold, $P(\alpha,\alpha^*)$ obeys the following Fokker-Planck equation:

$$\frac{\partial P}{\partial t}=-\frac{\partial}{\partial\alpha}\left[\frac{1}{2}(\mathcal{A}-\kappa)\alpha P-\frac{1}{2}\mathcal{B}|\alpha|^2\,\alpha P\right]$$
$$-\frac{\partial}{\partial\alpha*}\left[\frac{1}{2}(\mathcal{A}-\kappa)\alpha^*P-\frac{1}{2}\mathcal{B}|\alpha|^2\,\alpha^*P\right]+\mathcal{A}\frac{\partial^2P}{\partial\alpha\partial\alpha^*} \tag{121}$$

The steady-state solution of this equation is given by

$$P(\alpha,\alpha^*)=\mathcal{N}\exp\left[\frac{(\mathcal{A}-k)|\alpha|^2-\mathcal{B}|\alpha|^4/2}{2\mathcal{A}}\right] \tag{122}$$

where $\mathcal{N}$ is a normalization constant. The P representation can be rewritten in terms of the variables $x=\mathrm{Re}\ \alpha$ and $y=\mathrm{Im}\ \alpha$ as

$$P(x,y)=\mathcal{N}\exp\left[-\frac{G(x,y)}{K\sigma}\right] \tag{123}$$

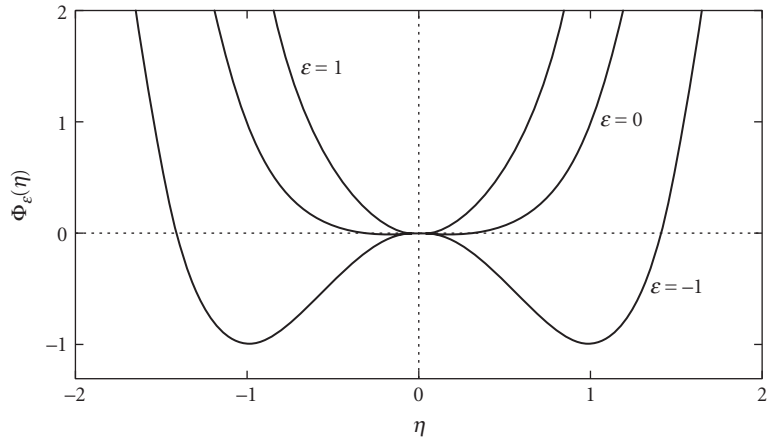

FIGURE 9 Scaled thermodynamical potentials. The $H = 0$ version of $F(M)$ and the $S = 0$ version of $G(E)$ can be expressed in terms of $\Phi_\varepsilon(\eta) = 2\varepsilon\eta^2 + \eta^4$ because

$$\Phi_\varepsilon(\eta) = \begin{cases} \dfrac{[F(M) - F_0]}{\dfrac{c^2 T_c}{4d}} & \text{with} \quad M = (c/d)^{1/2}(T/T_c)^{1/4}\eta \\ & \text{and} \quad \varepsilon = (T - T_c)/(TT_c)^{1/2} \\ \dfrac{[G(E) - G_0]}{\dfrac{a^2\sigma_t}{8b}} & \text{with} \quad E = (a/b)^{1/2}(\sigma_t/\sigma)^{1/4}\eta \\ & \text{and} \quad \varepsilon = (\sigma_t - \sigma)/(\sigma\sigma_t)^{1/2} \end{cases}$$

are equivalent to the respective entries in Table 1. The plot shows $\Phi_\varepsilon(\eta)$ for $\varepsilon = 1$ (ferromagnet above, T_c, laser below threshold), $\varepsilon = 0$ (ferromagnet at T_c, laser at threshold), and $\varepsilon = -1$ (ferromagnet below T_c, laser above threshold).

with

$$G(x, y) = -\frac{1}{4}a(\sigma - \sigma_t)(x^2 + y^2) + \frac{1}{8}b\sigma(x^2 + y^2)^2 \tag{124}$$

Here $K = a/4$ is one-fourth of the gain of one atom, $a(\sigma - \sigma_t) = \mathcal{A} - \kappa$, and $b\sigma = \mathcal{B}$.

We can see that the steady-state situation of the laser corresponds to the minimum value of G, i.e., $\partial G/\partial x = \partial G/\partial y = 0$. These solutions are $x = y = 0$ and $|\alpha|^2 = (x^2 + y^2) = a(\sigma - \sigma_t)/b\sigma$. Thus, for $(\sigma - \sigma_t) < 0$, the only allowed solution is $x = y = 0$. However, for $(\sigma - \sigma_t) > 0$, $x = y = 0$ is an unstable solution as the second derivative of G with respect to x and y is positive. This is seen clearly in Fig. 9, where we have plotted G versus $x = E$ for $y = 0$.

We thus see that G behaves in essentially the same way as the free energy of a thermodynamic system.

It should be emphasized that in the thermodynamic treatment of the ferromagnetic order-disorder transition, there are three variables required: (1) magnetization M, (2) external magnetic field H, and (3) temperature T. In order to have a complete analogy, it is important to realize that in addition to the electric-field-magnetization, population inversion-temperature correspondences, there must exist a further correspondence between the external magnetic field and a corresponding symmetry-breaking mechanism in the laser analysis. As shown in Ref. 111 and illustrated in Fig. 10, this symmetry breaking mechanism in the laser problem corresponds to an injected classical signal S. This leads to a skewed effective free energy.

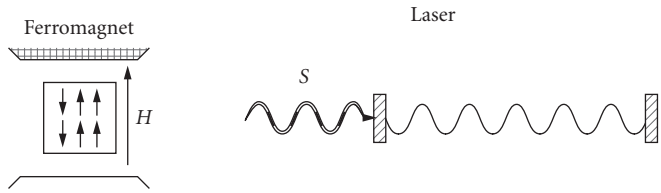

FIGURE 10 Figure depicting the broken symmetry mode of operation for both a ferromagnet and a laser.

An example of how the analogy can provide us with deeper insight is contained in the fact that we are able to *guess* correctly the $P(E)$ for a laser influenced by an injected signal, by analogy with the corresponding magnetic problem in the broken symmetry mode of operation.

More recently we have been turning the tables and using the quantum laser theory to learn about Bose-Einstein condensation (BEC). Recent experiments on BEC in laser-cooled gases,[112–114] and in He^4 in porous gel,[115] have stimulated a wealth of theoretical work[116–118] on the equilibrium and nonequilibrium properties of confined quantum degenerate gases.[119–124] Presently the partition function, critical temperature, and other such quantities are of interest for N bosons in a box below T_c. But the canonical ensemble is difficult to use in practice, because the state sums must be restricted to N particles. Indeed, the canonical partition function for a Bose gas of N particles at temperature T has not been so widely studied as one might have thought. To quote Herzog and Olshanii,

> To our knowledge there is no simple analytic expression for the canonical partition function in [the case of N bosons in a three-dimensional trap].[121]

Furthermore, there are questions of principle concerning the critical temperature and the validity of using phase-transition concepts in a mesoscopic sample having a small number of particles ($N \simeq 10^3$). In fact, Uhlenbeck pointed out to Einstein many years ago that BEC rigorously occurs only in the limit of infinite particle number.[125] Indeed, for a finite number of atoms there is no sharp "critical point " or critical temperature T_c. But the same can be said for the laser threshold. There is a *gradual* transition from disorder to order in both cases. However, as discussed later, even when fluctuations are present, T_c for a Bose gas and the laser threshold inversion are well defined.

Motivated by the preceding, we extend the laser-phase transition analogy to include BEC. We present a new approach to the problem of N bosons in thermal equilibrium below T_c. We emphasize that the present work provides another example[126] in which steady-state (detailed balance) solutions to nonequilibrium equations of motion provide a supplementary approach to conventional statistical mechanics (e.g., partition-function calculations). The present approach lends itself to different approximations; yielding, among other things, a simple (approximate) analytic expression for the ground-state density matrix for N trapped bosons and the partition function for same.

Thus, we seek a nonequilibrium equation of motion for the ground state of an ideal Bose gas in a three-dimensional harmonic trap coupled to the thermal reservoir, as shown elsewhere.[127]

$$\dot{\rho}_{n_0,n_0} = -K_{n_0}(n_0+1)\rho_{n_0,n_0} + K_{n_0-1}n_0\rho_{n_0-1,n_0-1} - H_{n_0}n_0\rho_{n_0,n_0} + H_{n_0+1}(n_0+1)\rho_{n_0+1,n_0+1} \tag{125}$$

The cooling and heating coefficients K_{n_0} and H_{n_0} are given by

$$K_{n_0} = \sum_k 2\pi W_k g_k^2 \langle \eta_k + 1 \rangle \langle n_k \rangle_{n_0} \tag{126}$$

and

$$H_{n_0} = \sum_k 2\pi W_k g_k^2 \langle \eta_k \rangle \langle n_k + 1 \rangle_{n_0} \tag{127}$$

where W_k is the heat-bath density of states, $\langle \eta_k \rangle$ is the average occupation number of the kth heat-bath oscillator, and $\langle \eta_k \rangle_{n_0}$ is the average number of atoms in the kth excited state, given n_0 atoms in the condensate. Here the coefficient K_{n_0} denotes the cooling rate from the excited states to the ground state, and similarly H_{n_0} stands for the heating rate for the ground state.

The heating term is approximately

$$H_{n_0} \simeq \kappa \sum_k \langle \eta(\varepsilon_k) \rangle = \kappa \sum_{\ell,m,n} \left[\exp\left(\frac{\hbar\Omega}{k_B T} \right) (\ell + n + m) - 1 \right]^{-1} \tag{128}$$

In the weak trap limit, this yields

$$H_{n_0} \simeq \kappa \left(\frac{k_B T}{\hbar\Omega} \right)^3 \zeta(3) \tag{129}$$

where $\zeta(3)$ is the Riemann zeta function and Ω is the trap frequency. Likewise, the cooling term in Eq. (125) is governed by the total number of excited state bosons,

$$K_{n_0} \simeq \kappa \sum_k \langle n_k \rangle_{n_0} = \kappa (N - n_0) \tag{130}$$

By writing the equation of motion for $\langle n_0 \rangle$ from Eq. (125), using H_{n_0} in the weak trap limit, and Eq. (130) for K_{n_0}, we find

$$\langle \dot{n}_0 \rangle = \kappa \left[(N+1) \langle n_0 \rangle - \langle (n_0 + 1)^2 \rangle - \zeta(3) \left(\frac{k_B T}{\hbar\Omega} \right)^3 \langle n_0 \rangle \right] + \kappa (N+1) \tag{131}$$

Noting that near T_c, $\langle n_0 \rangle = N$, we may neglect $\langle (n_0 + 1)^2 \rangle$ compared to $N \langle n_0 \rangle$, and neglecting the spontaneous emission term $\kappa(N+1)$, Eq. (131) becomes

$$\langle \dot{n}_0 \rangle = \kappa \left[N - \zeta(3) \left(\frac{k_B T}{\hbar\Omega} \right)^3 \right] \langle n_0 \rangle \tag{132}$$

We now define the critical temperature (in analogy with the laser threshold) such that cooling (gain) equals heating (loss) and $\langle \dot{n}_0 \rangle = 0$ at $T = T_c$; this yields

$$T_c = \left(\frac{\hbar\Omega}{k_B} \right) \left[\frac{N}{\zeta(3)} \right]^{1/3} \tag{133}$$

Thus, by defining the critical temperature as that temperature at which the rate of removal of atoms from the ground state equals the rate of addition, we arrive at the usual definition for the critical temperature, even for mesoscopic systems.

23.6 EXOTIC MASERS AND LASERS

Lasing without Inversion

For a long time, it was considered that population inversion was necessary for laser action to take place. Recently, it has been shown both theoretically[128–130] and experimentally[131–134] that it is also

QUANTUM THEORY OF THE LASER 23.41

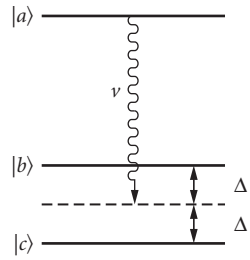

FIGURE 11 Level diagram for lasing without inversion.

possible to achieve lasing without inversion (LWI). In LWI, the essential idea is the cancellation of absorption by atomic coherence and interference.

Consider a system of three-level atoms interacting with a laser field in a cavity. The simple model we will focus on is that of Fig. 11. The atoms have one upper level $|a\rangle$ and two lower levels $|b\rangle$ and $|c\rangle$, with energies $\hbar\omega_a$, $\hbar\omega_b$, and $\hbar\omega_c$, respectively. The cavity field of frequency ν can be detuned from the atomic transition, as shown in the figure. The transitions $|a\rangle \rightarrow |b\rangle$ and $|a\rangle \rightarrow |c\rangle$ are now induced by one classical light field of frequency ν. The transition $|b\rangle \rightarrow |c\rangle$ is dipole forbidden. The atoms are pumped at a rate r_a in a coherent superposition of states

$$\rho(t_i) = \rho_{aa}^{(0)} |a\rangle\langle a| + \rho_{bb}^{(0)} |b\rangle\langle b| + \rho_{cc}^{(0)} |c\rangle\langle c| + \rho_{bc}^{(0)} |b\rangle\langle c| + \rho_{cb}^{(0)} |c\rangle\langle b| \tag{134}$$

Here $\rho_{\alpha\alpha}^{(0)} (\alpha = a, b, c)$ are the level populations and $\rho_{\alpha\alpha'}^{(0)} (\alpha \neq \alpha')$ are the atomic coherences. We give a simple argument to show how cancellation of absorption can lead to lasing without inversion in this scheme.

As the levels $|b\rangle$ and $|c\rangle$ are independent, the probability of emission is given by

$$\begin{aligned} P_{\text{emission}} &= P_b + P_c \\ &= (|\kappa_{a\rightarrow b}| 2\mathscr{E}^2 + |\kappa_{a\rightarrow c}| 2\mathscr{E}^2) \rho_{aa}^{(0)} \end{aligned} \tag{135}$$

where $\kappa_{a\rightarrow b}$ and $\kappa_{a\rightarrow c}$ are constants which depend on the matrix element between the relevant levels and the coupling of the atom with the field. On the other hand, the absorption probability is given by

$$\begin{aligned} P_{\text{absorption}} &= \kappa |C_b + C_c| 2\mathscr{E}^2 \\ &= \kappa (\rho_{bb}^{(0)} + \rho_{cc}^{(0)} + \rho_{bc}^{(0)} + \rho_{cb}^{(0)}) \mathscr{E}^2 \end{aligned} \tag{136}$$

where c_a and c_b are the probability amplitudes for the states $|b\rangle$ and $|c\rangle$. Therefore, the rate of growth of the laser field amplitude, under appropriate conditions, becomes

$$\dot{\mathscr{E}} = \frac{\mathscr{A}}{2} (\rho_{aa}^{(0)} - \rho_{bb}^{(0)} - \rho_{cc}^{(0)} - \rho_{bc}^{(0)} - \rho_{cb}^{(0)}) \mathscr{E} \tag{137}$$

Here $\mathscr{A}$ is a constant. Thus, if the terms $\rho_{bc}^{(0)}$ and $\rho_{cb}^{(0)}$ cancel $\rho_{bb}^{(0)}$ and $\rho_{cc}^{(0)}$, we have

$$\dot{\mathscr{E}} = \frac{\mathscr{A}}{2} \rho_{aa}^{(0)} \mathscr{E} \tag{138}$$

and we can have lasing even if only a small fraction of atoms is in the excited state $|a\rangle$, that is, even if $\rho_{aa} < (\rho_{bb} + \rho_{cc})$.

Physically, the lack of absorption in the three-level system considered here is a manifestation of quantum coherence phenomena. When an atom makes a transition from the upper level to the two lower levels, the total transition probability is the sum of $|a\rangle \rightarrow |b\rangle$ and $|a\rangle \rightarrow |c\rangle$ probabilities. However, the transition probability from the two lower levels to the single upper level is obtained by squaring the sum of the two probability amplitudes. When there is coherence between the two lower levels, this can lead to interference terms yielding a null in the transition probability corresponding to photon absorption.

Correlated (Spontaneous) Emission Laser

As discussed earlier, the fundamental source of noise in a laser is spontaneous emission. A simple pictorial model for the origin of the laser linewidth envisions it as being due to the random phase diffusion process arising from the addition of spontaneously emitted photons with random phases to the laser field. Here we show that the quantum noise leading to the laser linewidth can be suppressed below the standard Schawlow-Townes limit by preparing the atomic systems in a coherent superposition of states as in the Hanle-effect and quantum-beat experiments. In such coherently prepared atoms, the spontaneous emission is said to be *correlated*. Lasers operating via such a phase-coherent atomic ensemble are known as *correlated emission lasers* (CELs).[135]

An interesting aspect of the CEL is that it is possible to eliminate the spontaneous emission quantum noise in the relative linewidths by correlating the two spontaneous emission noise events.

A number of schemes exist in which quantum noise quenching below the standard limit can be achieved. In two-mode schemes a correlation between the spontaneous emission events in two different modes of the radiation field is established via atomic coherence so that the relative phase between them does not diffuse or fluctuate. In a Hanle laser[136] and a quantum-beat laser[137] this is achieved by pumping the atoms coherently such that every spontaneously emitting atom contributes equally to the two modes of the radiation, leading to a reduction and even vanishing of the noise in the phase difference. In a two-photon CEL, a cascade transition involving three-level atoms is coupled to only one mode of the radiation field.[138] A well-defined coherence between the upper and lower levels $|a\rangle$ and $|c\rangle$ leads to a correlation between the light emitted by an $|a\rangle \rightarrow |b\rangle$ and a subsequent $|b\rangle \rightarrow |c\rangle$ transition.

The quantum theory of quantum-beat or Hanle-effect lasers may be conveniently cast in terms of the equation of motion for the density matrix describing the laser radiation field $\rho(a_1, a_1^\dagger; a_2, a_2^\dagger)$; that is,

$$\dot{\rho} = \sum_{ij} \mathcal{L}_{ij} \rho \tag{139}$$

where the linear gain and cross-coupling Liouville operators are given by

$$\mathcal{L}_{ii}\rho = -\frac{1}{2}[\alpha_{ii}\rho a_i a_i^\dagger + \alpha_{ii}^* a_i a_i^\dagger \rho - (\alpha_{ii} + \alpha_{ii}^*) a_i^\dagger \rho a_i] \tag{140}$$

$$\mathcal{L}_{12}\rho = -\frac{1}{2}[\alpha_{12}\rho a_2 a_1^\dagger + \alpha_{21}^* a_2 a_1^\dagger \rho - (\alpha_{12} + \alpha_{21}^*) a_1^\dagger \rho a_2] e^{i\Phi} \tag{141}$$

$$\mathcal{L}_{21}\rho = -\frac{1}{2}[\alpha_{21}\rho a_1 a_2^\dagger + \alpha_i^* a_1 a_2^\dagger \rho - (\alpha_i + \alpha_i^*) a_2^\dagger \rho a_1] e^{i\Phi} \tag{142}$$

Here α_{ij} are constants that depend on the parameters of the gain medium such as detunings, Rabi frequency of the driving field, and so on. When the coherent mixing of levels $|a\rangle$ and $|\mathrm{b}\rangle$ is produced via a microwave signal having frequency ω_0, the phase angle ϕ is given by $\Phi(t) = (\nu_1 - \nu_2 - \omega_0)t - \phi$ where ϕ is the (microwave determined) atomic-phase difference $\phi_a - \phi_b$. In the case of polarization-induced

coherent mixing, the phase angle is $\Phi(t)=(\nu_2-\nu_2)t-\phi$, where ϕ is again the relative phase between levels $|a\rangle$ and $|b\rangle$ but determined this time by the state of elliptic polarization of the pump light used to excite the atoms.

The Liouville equation (31) for the reduced-density operator for the field can be converted into an equivalent Fokker-Planck equation by introducing coherent state representation for a_1 and a_2 and the P representation $P(\alpha, \alpha^*)$ for ρ. If we define the coherent states as

$$a_i\ |\alpha_1, \alpha_2|\rangle=\alpha_i\,|\alpha_1, \alpha_2|\rangle; i=1, 2 \tag{143}$$

where α is an arbitrary complex number, and we represent α_i as

$$\alpha_i=\rho_i \exp(i\theta_i); i=1, 2 \tag{144}$$

then the Fokker-Planck equation in terms of ρ_i, θ_i will contain a term which describes diffusion of relative phase $\theta=\theta_1-\theta_2$ as

$$\dot{P}=\frac{\partial^2}{\partial\theta^2}[\mathcal{D}(0)P] \tag{145}$$

with

$$\mathcal{D}=\frac{1}{16}\left\{\left(\frac{\alpha_{11}}{\rho_1^2}+\frac{\alpha_{22}}{\rho_2^2}\right)-\frac{(\alpha_{12}+\alpha_{21}^*)e^{-i\psi}}{\rho_1\rho_2}\right\} \tag{146}$$

and $\psi=\Phi+\theta_1-\theta_2$ with θ_i being the phase of the ith field. The diffusion constant $\mathcal{D}$ for the relative phase vanish for $\psi=0$, $\rho_1=\rho_2$, and $\alpha_{11}=\alpha_{22}=\alpha_{12}=\alpha_{21}^*$, thus leading to CEL action.

Free-Electron Laser

A coherent emission of radiation in a free-electron laser (FEL) is due to the bunching of a relativistic electron beam propagating along a periodic magnetic structure. The electrons experience a Lorentz force and thus follow oscillating orbits and radiate. This spontaneous emission coupled with the periodic magnetic structure give rise to a periodic ponderomotive potential. The electrons bunch together and radiate coherently.[139] The spontaneous emission pattern of a relativistic electron of energy $E=\gamma mc^2$ with $\gamma\gg1$ is mostly in the forward direction. For a magnetic wiggler of period λ_W, the spectrum in the forward direction is symmetric about the wavelength $\lambda_s\cong\lambda_W/2\gamma^2$. Thus, a change of the periodicity of the wiggler λ_W can be used to tune the coherent light emitted by the FEL over a very wide range.

Many interesting features of FEL can be understood classically. However, the quantum-statistical properties of radiation emitted by FEL exhibit many interesting features such as squeezing and sub-poissonian statistics.[140–142]

Here we describe a free-electron amplifier in the small-signal noncollective regime. Such an FEL can be described by the one-electron nonrelativistic Bambini-Renieri hamiltonian which refers to a moving frame, where the laser and the wiggler frequencies coincide with $\omega=ck/2$.[143] In this frame, resonance occurs when the electron is at rest; therefore, the electron can be treated nonrelativistically. The hamiltonian is given by

$$\mathcal{H}=\frac{p^2}{2m}+\hbar\omega A^\dagger A+i\hbar g(A-A^\dagger) \tag{147}$$

with $A = a \exp(ikz)$. Here a is the annihilation operator of the laser field, p and z are the electron's momentum and coordinate with $[z, p] = i\hbar$, $[A, A^\dagger] = 1$, $[p, A] = \hbar kA$, m is the effective mass of the electron, and

$$g = \left(\frac{e^2 B}{mk}\right)\left(\frac{2}{V\varepsilon_0 \hbar\omega}\right)^{1/2} \tag{148}$$

with V the quantization volume and B the magnetic-field strength of the wiggler field in the moving frame. In Eq. (147) we have already taken the classical limit of the wiggler field. By transforming to the interaction picture we obtain

$$\mathcal{H}_I = ig\hbar\left\{\exp\left[-\frac{it(\hbar k^2 + 2kp)}{2m}\right]A^\dagger - Hc\right\} \tag{149}$$

We now consider an initial state made up by an electron with momentum p and the field vacuum, i.e., $|\text{in}\rangle = \overline{p}|\overline{p}, 0\rangle$

$$p|\overline{p}, 0\rangle = \overline{p}\,|\overline{p}, 0\rangle \tag{150}$$

$$A|\overline{p}, 0\rangle = 0 \tag{151}$$

$$A^\dagger|\overline{p}, 0\rangle = |\overline{p} - \hbar k, 1\rangle \tag{152}$$

The final-state expectation value of any operator $O(A, A^\dagger)$ is then

$$\langle \text{out}|O|\text{out}\rangle = \langle \overline{p}, 0|\overline{s}^\dagger(T)OS(T)|\overline{p}, 0\rangle \tag{153}$$

where

$$S(T) = T\exp\left[-\frac{i}{\hbar}\int_{-T/2}^{T/2} dt\, H_I(t)\right] \tag{154}$$

is the time-evolution operator for the electron-photon state.

The evaluation of Eq. (153) is straightforward in the small-signal limit along the lines given in Ref. 141, and we obtain

$$(\Delta A_1)^2 = \frac{1}{4} - \frac{\hbar k^2}{2m} j\frac{\partial j}{\partial \beta} \tag{155a}$$

$$(\Delta A_1)^2 = \frac{1}{4} + \frac{\hbar k^2}{2m} j\frac{\partial j}{\partial \beta} \tag{155b}$$

$$(\Delta A_1)(\Delta A_2) = \frac{1}{4} \tag{155c}$$

$$\Delta n^2 - \langle n\rangle = -\frac{2\hbar k^2}{m} j^3\frac{\partial j}{\partial \beta} \tag{155d}$$

where

$$j = \left(\frac{2g}{\beta}\right)\sin\left(\frac{\beta T}{2}\right) \tag{156}$$

$$\beta = \frac{k\overline{p}}{m} \tag{157}$$

In our notation, the gain of the free-electron laser is proportional to $-j\partial j/\partial\beta$. Hence, Eqs. (155*a*) and (155*b*) show that, depending on the sign of the gain, either A_1 or A_2 is squeezed while, because of Eq. (155*c*), minimum uncertainty is maintained. Here, we have defined squeezing with respect to the operator A instead of the annihilation operator a of the radiation field. This must be so because we employ electron-photon states, and the annihilation of a photon always comes up to increasing the momentum of the electron by $\hbar k$. Finally, Eq. (155*d*) shows that we have subpoissonian, poissonian, or superpoissonian statistics if the electron momentum is below resonance ($\beta<0$), at resonance ($\beta=0$), or below resonance ($\beta>0$), respectively.

Exploiting the Quantized Center-of-Mass Motion of Atoms

In the treatment of the interaction of a two-level atom with photons of a single, dynamically privileged mode by the Jaynes-Cummings model, as discussed in Sec. 23.4, the center-of-mass motion of the atom is regarded as classical. This is a well-justified approximation, since the atom's kinetic energy of typically $\sim 10^{-2}$ eV is many orders of magnitude larger than the interaction energy of typically $\sim 10^{-11}$ eV if the atom belongs to a thermal beam. For ultracold atoms, however, matters can be quite different, and the quantum properties of the center-of-mass motion must be taken into account.

Early studies showed that very slow atoms can be reflected at the entry port of a resonator[144] or trapped inside.[145] The reflection probability is considerable even if the photon lifetime is not short as compared with the relatively long interaction time.[146]

Whereas Refs. 144 to 146 deal mainly with the mechanical effects on the center-of-mass motion of the atom, the modifications in the maser action are addressed in Refs. 147 to 150. For thermal atoms, the emission probability displays the usual Rabi oscillations (see Sec. 23.4) as a function of the interaction *time*. For very slow atoms, however, the emission probability is a function of the interaction *length* and exhibits resonances such as the ones observed in the intensity transmitted by a Fabry-Perot resonator. The resonances occur when the resonator length is an integer multiple of half the de Broglie wavelength of the atom inside the cavity.

A detailed calculation[147] shows that the emission probability is 50 percent at a resonance, irrespective of the number of photons that are present initially. Owing to this unusual emission probability, a beam of ultracold atoms can produce unusual photon distributions, such as a shifted thermal distribution. In the trilogy (Refs. 148 to 150) this *microwave amplification by z-motion-induced emission of radiation* (mazer) is studied in great detail.

In order to see the mazer resonances for atoms with a certain velocity spread, the interaction length has to be small. Therefore, micromaser cavities of the usual cylindrical shape, for which the smallest cavity length is given by half the wavelength of the microwaves, cannot be used for this purpose. But cavities of the reentrant type (familiar as components of klystrons) allow for an interaction length that is much smaller than the wavelength. With such a device, an experiment with realistic parameters seems possible.[149] As a potential application, we mention that a working mazer could be used as a velocity filter for atoms.[151]

23.7 ACKNOWLEDGMENTS

The authors gratefully acknowledge the generous support of the Office of Naval Research over the many years spent on completing the works reviewed here. It is also a pleasure to acknowledge the Max-Planck-Institute for Quantum Optics (Garching, Germany) for providing the excellent working atmosphere and the intellectual stimulus for the most interesting works in this field.

23.8 REFERENCES

1. J. R. Klauder and E. C. G. Sudarshan, *Fundamentals of Quantum Optics* (W. A. Benjamin, New York, 1970).
2. R. Loudon, *The Quantum Theory of Light* (Oxford University Press, New York, 1973).
3. W. H. Louisell, *Quantum Statistical Properties of Radiation* (John Wiley, New York, 1973).
4. H. M. Nussenzveig, *Introduction to Quantum Optics* (Gordon and Breach, New York, 1974).
5. M. Sargent III, M. O. Scully, and W. E. Lamb, Jr., *Laser Physics* (Addison-Wesley, Reading, Mass., 1974).
6. L. Allen and J. H. Eberly, *Optical Resonance and Two-Level Atoms* (John Wiley, New York, 1975).
7. H. Haken, *Light*, Vols. I and II (North-Holland, Amsterdam, 1981).
8. P. L. Knight and L. Allen, *Concepts of Quantum Optics* (Pergamon Press, Oxford, 1983).
9. P. Meystre and M. Sargent III, *Elements of Quantum Optics* (Springer-Verlag, Berlin, 1990).
10. C. W. Gardiner, *Quantum Noise* (Springer-Verlag, Berlin, 1991).
11. C. Cohen-Tannoudji, J. Dupont-Roc, and G. Grynberg, *Atom-Photon Interactions* (John Wiley, New York, 1992).
12. H. Carmichael, *An Open Systems Approach to Quantum Optics* (Springer-Verlag, Berlin, 1993).
13. W. Vogel and D.-G. Welsch, *Lectures on Quantum Optics* (Akademie Verlag, Berlin, 1994).
14. J. Peřina, Z. Hradil, and B. Jurčo, *Quantum Optics and Fundamentals of Physics* (Kluwer, Dordrecht, Netherlands, 1994).
15. D. F. Walls and G. J. Milburn, *Quantum Optics* (Springer-Verlag, Berlin, 1994).
16. L. Mandel and E. Wolf, *Optical Coherence and Quantum Optics* (Cambridge University Press, London, 1995).
17. E. R. Pike and S. Sarkar, *Quantum Theory of Radiation* (Cambridge University Press, London, 1995).
18. M. O. Scully and M. S. Zubairy, *Quantum Optics* (Cambridge University Press, London, 1997).
19. M. Planck, *Verh. Phys. Ges.* **2**:202, 237 (1900).
20. W. Wien, *Ann. Physik* **58**:662 (1896).
21. Lord Rayleigh, *Phil. Mag.* **49**:539 (1900).
22. J. H. Jeans, *Phil. Mag.* **10**:91 (1905).
23. A. H. Compton, *Phys. Rev.* **21**:483 (1923).
24. A. Einstein, *Ann. Physik* **17**:132 (1905).
25. W. Pauli, "Einstein's Contributions to Quantum Theory," in *Albert Einstein: Philosopher-Scientist,* P. A. Schilpp (ed.) (Library of Living Philosophers, Evanston, Ill., 1949).
26. L. de Broglie, *C. R. Acad. Sci. Paris* **177**:517 (1923).
27. L. de Broglie, *These* (Masson et Cie., Paris, 1924).
28. E. Schrödinger, *Ann. Physik* **79**:361 (1926).
29. G. I. Taylor, *Proc. Camb. Phil. Soc.* **15**:114 (1909).
30. P. A. M. Dirac, *The Principles of Quantum Mechanics,* 4th ed. (Oxford University Press, Oxford, 1958).
31. R. J. Glauber, *Am. I. Phys.* **63**:12 (1995).
32. A. Einstein, *Phys. Z.* **10**:185 (1909).
33. N. Bohr, *Phil. Mag.* **26**:1,476, 857 (1913).
34. A. Einstein, *Phys. Z.* **18**:121 (1917).
35. A. Einstein, *Ann. Physik* **17**:549 (1905).
36. N. Bohr, H. A. Kramers, and I. C. Slater, *Phil. Mag.* **47**:785 (1924).
37. W. Bothe and H. Geiger, *Z. Phys.* **26**:44 (1924).
38. S. N. Bose, *Z. Phys.* **26**:178 (1924).
39. S. N. Bose, *Z. Phys.* **27**:384 (1924).
40. A. Einstein, "Quantentheorie des einatomigen Gases," in *Sitzungsber. Preuss. Akad. Wiss., Phys.-math. Kl.,* 1924, p. 261.

41. A. Einstein, "Quantentheorie des einatomigen Gases. 2. Abhandlung," in *Sitzungsber. Preuss. Akad. Wiss, Phys.-math. Kl.,* 1925, p. 3.
42. A. Einstein, "Quantentheorie des idealen Gases," in *Sitzungsber. Preuss. Akad. Wiss., Phys.-math. Kl.,* 1925, p. 18.
43. P. A. M. Dirac, *Proc. Roy. Soc. London* **A114**:710 (1927).
44. J. Schwinger (ed), *Quantum Electrodynamics* (Dover, New York, 1958).
45. E. Fermi, *Rend. Lincei* **10**:72 (1929).
46. R. J. Glauber, *Phys. Rev.* **130**:2529 (1963).
47. R. J. Glauber, *Phys. Rev.* **131**:2766 (1963).
48. R. J. Glauber, *Phys. Rev. Lett.* **10**:84 (1963).
49. V. F. Weisskopf and E. P. Wigner, *Z. Phys.* **63**:47 (1930).
50. V. F. Weisskopf, *Phys. Rev.* **56**:72 (1939).
51. W. E. Lamb, Jr., and R. C. Retherford, *Phys. Rev.* **72**:241 (1947).
52. J. Schwinger, *Phys. Rev.* **73**:416 (1948).
53. S. Pasternack, *Phys. Rev.* **54**:1113 (1938).
54. S. Millman and P. Kusch, *Phys. Rev.* **57**:438 (1940).
55. H. Hanbury-Brown and R. Q. Twiss, *Phil. Mag.* **45**:663 (1954).
56. H. Hanbury-Brown and R. Q. Twiss, *Nature* (London) **178**:1046 (1956).
57. H. Hanbury-Brown and R. Q. Twiss, *Proc. Roy. Soc.* **A242**:300 (1957).
58. R. G. Newton, *Scattering Theory of Waves and Particles* (McGraw-Hill, New York, 1966).
59. C. K. Hong, Z. Y. Ou, and L. Mandel, *Phys. Rev. Lett.* **59**:2044 (1987).
60. P. G. Kwiat, K. Mattle, H. Weinfurter, and A. Zeilinger, *Phys. Rev. Lett.* **75**:4337 (1995).
61. P. G. Kwiat, E. Waks, A. G. White, I. Appelbaum, and P. H. Eberhard, *Phys. Rev. A* **60**:773 (1999).
62. D. Bouwmeester, J.-W. Pan, K. Mattle, M. Eibl, H. Weinfurter, and A. Zeilinger, *Nature* (*London*) **390**:575 (1997).
63. D. Boschi, S. Branca, F. De Martini, L. Hardy, and S. Popescu, *Phys. Rev. Lett.* **80**:1121 (1998).
64. C. H. Bennett, G. Brassard, C. Crepeau, R. Josza, A. Peres, and W. Wootters, *Phys. Rev. Lett.* **70**:1895 (1993).
65. K. Mattle, H. Weinfurter, P. G. Kwiat, and A. Zeilinger, *Phys. Rev. Lett.* **76**:4656 (1996).
66. C. H. Bennett and S. J. Wiesner, *Phys. Rev. Lett.* **69**:2881 (1992).
67. M. Sargent, M. O. Scully, and W. E. Lamb, *Laser Physics* (Addison-Wesley, Reading, Mass., 1974).
68. M. O. Scully and M. S. Zubairy, *Quantum Optics* (Cambridge University Press, Cambridge, 1997).
69. M. Lax, "Phase Noise in a Homogeneously Broadened Maser," in *Physics of Quantum Electronics,* P. L. Kelley, B. Lax, and P. E. Tannenwald (eds.) (McGraw-Hill, New York, 1966).
70. M. Lax, *Phys. Rev.* **145**:110 (1966).
71. M. Lax, "Fluctuations and Coherence Phenomena in Classical and Quantum Physics," in *1966 Brandeis Summer Lecture Series on Statistical Physics,* Vol. 2, M. Chretien, E. P. Gross, and S. Dreser (eds.) (Gordon and Breach, New York, 1968; Mir, Moscow, 1975).
72. W. H. Louisell, *Quantum Statistical Properties of Radiation* (John Wiley, New York, 1973).
73. H. Haken, "Laser Theory," in *Encyclopedia of Physics,* Vol. 35/c, S. Flügge (ed.) (Springer, Berlin, 1970).
74. H. Risken, *The Fokker Planck Equation* (Springer, Heidelberg, 1984).
75. M. Lax, "The Theory of Laser Noise," keynote address, 1990 Conference on Laser Science and Optics. Applications, *Proc. SPIE* **1376**:2 (1991).
76. E. T. Jaynes and F. W. Cummings, *Proc. IEEE* **51**:89 (1963).
77. B. W. Shore and P. L. Knight, *J. Mod. Opt.* **40**:1195 (1993).
78. J. P. Gordon, H. J. Zeiger, and C. H. Townes, *Phys. Rev.* **95**:282L (1955).
79. J. P. Gordon, H. J. Zeiger, and C. H. Townes, *Phys. Rev.* **99**:1264 (1955).
80. A. L. Schawlow and C. H. Townes, *Phys. Rev. A* **112**:1940 (1958).
81. N. G. Basov and A. M. Prokhorov, *Dokl. Ak. Nauk* **101**:47 (1955).

82. T. H. Maiman, *Nature* (London) **187**:493 (1960).
83. A. Javan, W. R. Bennett, and D. R. Herriott, *Phys. Rev. Lett.* **6**:106 (1961).
84. W. E. Lamb, *Phys. Rev.* **134**:A1429 (1964).
85. For recent reviews, see, e.g., B.-G. Englert, M. Löffler, O. Benson, B. Varcoe, M. Weidinger, and H. Walther, *Fortschr. Phys.* **46**:897 (1998); G. Raithel, C. Wagner, H. Walther, L. M. Narducci, and M. O. Scully, in *Advances in Molecular and Optical Physics,* P. Berman (ed.) (Academic, New York, 1994), Suppl. 2.
86. D. Meschede, H. Walther, and G. Müller, *Phys. Rev. Lett.* **54**:551 (1985).
87. P. Filipowicz, J. Javanainen, and P. Meystre, *Phys. Rev. A* **34**:3077 (1986).
88. M. Lax, *Phys. Rev.* **129**:2342 (1963).
89. M. Lax and M. Zwanziger, *Phys. Rev. A* **7**:750 (1973).
90. M. Lax, *Phys. Rev.* **172**:350 (1968).
91. N. Lu, *Phys. Rev. A* **47**:4322 (1993).
92. U. Herzog and J. Bergou, *Phys. Rev. A* **62** (2000). In press.
93. M. Lax, *Phys. Rev.* **160**:290 (1967).
94. R. D. Hempstead and M. Lax, *Phys. Rev.* **161**:350 (1967).
95. H. Risken and H. D. Vollmer, *Z. Physik* **191**:301 (1967).
96. M. Kac, in *1966 Brandeis Summer Lecture Series on Statistical Physics,* Vol. 1, M. Chretien, E. P Gross, and S. Dreser (eds.) (Gordon and Breach, New York, 1968).
97. M. O. Scully, H. Walther, G. S. Agarwal, T. Quang, and W. Schleich, *Phys.* Rev. *A* **44**:5992 (1991).
98. N. Lu, *Phys. Rev. Lett.* **70**:912 (1993); N. Lu, *Phys. Rev. A* **47**:1347 (1993); T. Quang, G. S. Agarwal, J. Bergou, M. O. Scully, H. Walther, K. Vogel, and W. P. Schleich, *Phys. Rev. A* **48**:803 (1993); K. Vogel, W. P. Schleich, M. O. Scully, and H. Walther, *Phys. Rev. A* **48**:813 (1993); R. McGowan and W. Schieve, *Phys. Rev. A* **55**:3813 (1997).
99. S. Qamar and M. S. Zubairy, *Phys. Rev. A* **44**:7804 (1991).
100. P. Filipowicz, J. Javanainen, and P. Meystre, *J. Opt. Soc. Am. B* **3**:154 (1986).
101. J. J. Slosser, P. Meystre, and S. L. Braunstein, *Phys. Rev. Lett.* **63**:934 (1989).
102. J. Bergou, L. Davidovich, M. Orszag, C. Benkert, M. Hillery, and M. O. Scully, *Phys. Rev. A* **40**:7121 (1989); J. D. Cresser, *Phys. Rev. A* **46**:5913 (1992); U. Herzog, *Phys. Rev. A* **52**:602 (1995).
103. H. J. Briegel, B.-G. Englert, N. Sterpi, and H. Walther, *Phys. Rev. A* **49**:2962 (1994); U. Herzog, *Phys. Rev. A* **50**:783 (1994); J. D. Cresser and S. M. Pickless, *Phys. Rev. A* **50**:R925 (1994); U. Herzog, *Appl. Phys. B* **60**:S21 (1995).
104. H.-J. Briegel, B.-G. Englert, Ch. Ginzel, and A. Schenzle, *Phys. Rev. A* 49:5019 (1994).
105. H.-J. Briegel, B.-G. Englert, *Phys. Rev. A* **52**:2361 (1995); J. Bergou, *Quantum and Semiclass. Optics* **7**:327 (1995); U. Herzog and J. Bergou, *Phys. Rev. A* **54**:5334 (1996); ibid. **55**:1385 (1997).
106. M. Weidinger, B. T. H. Varcoe, R. Heerlein, and H. Walther, *Phys. Rev. Lett.* **82**:3795 (1999).
107. H. Walther, *Phys. Rep.* **219**:263 (1992).
108. M. O. Scully, G. Süssmann, and C. Benkert, *Phys. Rev. Lett.* **60**:1014 (1988).
109. M. O. Scully, M. S. Zubairy, and K. Wódkiewicz, *Opt. Commun.* **65**:440 (1988).
110. H. E. Stanley, *Introduction to Phase Transitions and Critical Phenomema* (Oxford University Press, Oxford, 1971).
111. V. DeGiorgio and M. O. Scully, *Phys. Rev. A* **2**:1170 (1970).
112. M. Anderson, J. Ensher, M. Matthews, C. Wieman, and E. Cornell, *Science* **269**:198 (1995).
113. C. Bradley, C. Sackett, J. Tollett, and R. Hulet, *Phys. Rev. Lett.* **75**:1687 (1995).
114. K. Davis, M. Mewes, M. Andrews, N. van Druten, D. Durfee, D. Kurn, and W. Ketterle, *Phys. Rev. Lett.* **75**:3969 (1995).
115. M. H. W. Chen, K. I. Blum, S. Q. Murphy, G. K. S. Wong, and J. D. Reppy, *Phys. Rev. Lett.* **61**:1950 (1998).
116. K. Huang, *Statistical Mechanics* (John Wiley, New York, 1987).
117. R. Arnowitt and M. Girardeau, *Phys. Rev.* **113**:745 (1959).

118. G. Baym and C. Pethick, *Phys. Rev. Lett.* **76**:6 (1996).
119. H. Politzer, *Phys. Rev. A* **54**:5048 (1996).
120. S. Grossmann and M. Holthaus, *Phys. Rev. E* **54**:3495 (1996).
121. C. Herzog and M. Olshanii, *Phys. Rev. A* **55**:3254 (1997).
122. P. Navez, D. Bitouk, M. Gajda, Z. Idziaszek, and K. Rzążewski, *Phys. Rev. Lett.* **79**:1789 (1997).
123. M. Wilkens and C. Weiss, J. *Mod. Opt.* **44**:1801 (1997).
124. S. Grossmann and M. Holthaus, *Phys. Rev. Lett.* **79**:3557 (1997).
125. H. Woolf (ed.), *Some Strangeness in the Proportion: A Centennial Symposium to Celebrate the Achievements of Albert Einstein* (Addison-Wesley, Reading, Mass., 1980), p. 524.
126. J. Goldstein, M. O. Scully, and P. Lee, *Phys. Lett.* **A35**:317 (1971).
127. M. O. Scully, *Phys. Rev. Lett.* **82**:3927 (1999).
128. O. Kocharovskaya and Ya I. Khanin, *JETP Lett.* **48**:630 (1988).
129. S. E. Harris, *Phys. Rev. Lett.* **62**:1033 (1989).
130. M. O. Scully, S.-Y. Zhu, and A. Gavrieleides, *Phys. Rev. Lett.* **62**:2813 (1989).
131. A. Nottelmann, C. Peters, and W. Lange, *Phys. Rev. Lett.* **70**:1783 (1993).
132. E. S. Fry, X. Li, D. Nikonov, G. G. Padmabandu, M. O. Scully, A. V. Smith, F. K. Tittel, C. Wang, S. R. Wilkinson, and S.-Y. Zhu, *Phys. Rev. Lett.* **70**:3235 (1993).
133. W. E. van der Veer, R. J. J. van Diest, A. Dönszelmann, and H. B. van Linden van den Heuvell, *Phys. Rev. Lett.* **70**:3243 (1993).
134. A. S. Zibrov, M. D. Lukin, D. E. Nikonov, L. W. Hollberg, M. O. Scully, V. L. Velichansky, and H. G. Robinson, *Phys. Rev. Lett.* **75**:1499 (1995).
135. M. O. Scully, *Phys. Rev. Lett.* **55**:2802 (1985).
136. J. Bergou, M. Orszag, and M. O. Scully, *Phys. Rev. A* **38**:768 (1988).
137. M. O. Scully and M. S. Zubairy, *Phys. Rev. A* **35**:752 (1987).
138. M. O. Scully, K. Wodkiewicz, M. S. Zubairy, J. Bergou, N. Lu, and J. Meyer ter Vehn, *Phys. Rev. Lett.* **60**:1832 (1988).
139. J. M. J. Madey, *J. Appl. Phys.* **42**:1906 (1971).
140. W. Becker, M. O. Scully, and M. S. Zubairy, *Phys. Rev. Lett.* **48**:475 (1985).
141. W. Becker and M. S. Zubairy, *Phys. Rev. A* **25**:2200 (1982).
142. R. Bonifacio, *Opt. Commun.* **32**:440 (1980).
143. A. Bambini and A. Renieri, *Opt. Commun.* **29**:244 (1978).
144. B.-G. Englert, J. Schwinger, A. O. Barut, and M. O. Scully, *Europhys. Lett.* **14**:25 (1991).
145. S. Haroche, M. Brune, and J.-M. Raimond, *Europhys. Lett.* **14**:19 (1991).
146. M. Battocletti and B.-G. Englert, *J. Phys. II France* **4**:1939 (1994).
147. M. O. Scully, G. M. Meyer, and H. Walther, *Phys. Rev. Lett.* **76**:4144 (1996).
148. G. M. Meyer, M. O. Scully, and H. Walther, *Phys. Rev. A* **56**:4142 (1997).
149. M. Löffler, G. M. Meyer, M. Schröder, M. O. Scully, and H. Walther, *Phys. Rev. A* **56**:4153 (1997).
150. M. Schröder, K. Vogel, W. P. Schleich, M. O. Scully, and H. Walther, *Phys. Rev. A* **56**:4164 (1997).
151. M. Löffler, G. M. Meyer, and H. Walther, *Lett.* **41**:593 (1998).